Export fluxes in a naturally iron-fertilized area of the Southern Ocean: seasonal dynamics of particulate organic carbon export from a moored sediment trap (part 1).

M. Rembauville[1,2] , I. Salter[1,2,3] , N. Leblond[4,5] , A. Gueneugues[1,2] and S. Blain[1,2]

[1] Sorbonne Universités, UPMC Univ Paris 06, UMR 7621, LOMIC, Observatoire Océanologique, Banyuls-sur-Mer, France.

[2] CNRS, UMR 7621, LOMIC, Observatoire Océanologique, Banyuls-sur-Mer, France.

[3] Alfred-Wegener-Institute for Polar and Marine research, Bremerhaven, Germany.

[4]Sorbonne Universités, UPMC Univ Paris 06, LOV, UMR 7093, Observatoire Océanologique, Villefranche-sur-Mer, France

[5]CNRS-INSU, LOV, UMR 7093, Observatoire Océanologique, Villefranche-sur-Mer, France

Correspondance to: M. Rembauville (rembauville@obs-banyuls.fr).

Abstract

A sediment trap moored in the naturally iron-fertilized Kerguelen plateau in the Southern Ocean provided an annual record of particulate organic carbon and nitrogen fluxes at 289 m. At the trap deployment depth current speeds were typically low (~10 cm s^{-1}) and primarily tidal-driven (M2 tidal component). Although advection was weak, the sediment trap may have been subject to hydrodynamical and biological (swimmer feeding on trap funnel) biases that could explain the collection of only 15-30 % of the ^{234}Th derived flux. Particulate organic carbon (POC) flux was generally low (<0.5 mmol m^{-2} d^{-1}) although two episodic export events (<14 days) of 1.5 mmol m^{-2} d^{-1} were recorded. These increases in flux occurred with a 1-month time lag from peaks in surface chlorophyll and together accounted for approximately 40 % of the annual flux budget. The annual POC flux of 98.2±4.4 mmol m^{-2} y^{-1} was low

considering the shallow deployment depth, but comparable to independent estimates made at similar depths (~300 m) over the plateau and to deep-ocean (>2 km) fluxes measured from similarly productive iron-fertilized blooms. Although undertrapping cannot be excluded in shallow moored sediment trap deployment, we hypothesize that grazing pressure, including mesozooplankton and mesopelagic fishes, may be responsible for the large reduction in POC flux beneath the base of the winter mixed layer. The importance of plankton community structure in controlling the temporal variability of export fluxes is addressed in a companion paper.

1 Introduction

The biological carbon pump is defined as the vertical transfer of biologically fixed carbon in the ocean surface to the ocean interior (Volk and Hoffert, 1985). Global estimates of Particulate Organic Carbon (POC) export cluster between 5 Pg C y^{-1} (Moore et al., 2004; Lutz et al., 2007; Honjo et al., 2008; Henson et al., 2011; Lima et al., 2014a) to 10 Pg C y^{-1} (Laws et al., 2000; Schlitzer, 2004; Gehlen et al., 2006; Boyd and Trull, 2007; Dunne et al., 2007; Laws et al., 2011). The physical transfer of dissolved inorganic carbon to the ocean interior during subduction of water masses is two orders of magnitude higher (> 250 Pg C y^{-1}, Karleskind et al., 2011; Levy et al., 2013). The global ocean represents a net annual CO_2 sink of 2.5 Pg C y^{-1} (Le Quéré et al., 2013), slowing down the increase of the atmospheric CO_2 concentration resulting from anthropogenic activity. Although the Southern Ocean (south of 44°S) plays a limited role in the net air-sea CO_2 flux (Lenton et al., 2013), it is a key component of the global anthropogenic CO_2 sink representing one third the global oceanic sink (~1 Pg C y^{-1}) while covering 20 % of its surface (Gruber et al., 2009). The solubility pump is considered as the major component of this sink, whereas the biological carbon pump is considered to be inefficient in the Southern Ocean and sensitive to iron supply.

Following "the iron hypothesis" in the nineties (Martin 1990), iron limitation of high nutrient low chlorophyll (HNLC) areas, including the Southern Ocean, has been tested in bottle experiments (de Baar et al., 1990) and through *in situ* artificial fertilization experiments (de Baar et al., 2005; Boyd et al., 2007). Results from these experiments are numerous and essentially highlight that iron limits macronutrient (N, P, Si) utilization (Boyd et al., 2005; Hiscock and Millero, 2005) and primary production (Landry et al., 2000; Gall et al., 2001; Coale et al., 2004) in these vast HNLC areas of the Southern Ocean. Due to a large macronutrient repository the biological carbon pump in the Southern Ocean is considered to be inefficient in its capacity to transfer atmospheric carbon to the ocean interior (Sarmiento

66 and Gruber, 2006). In the context of micronutrient limitation, sites enriched in iron by natural
67 processes have also been studied and include the Kerguelen islands (Blain et al., 2001, 2007),
68 the Crozet islands (Pollard et al., 2007), the Scotia Sea (Tarling et al., 2012), and the Drake
69 Passage (Measures et al., 2013). Enhanced primary producer biomass in association with
70 natural iron supply (Korb and Whitehouse, 2004; Seeyave et al., 2007; Lefèvre et al., 2008)
71 strongly support trace-metal limitation. Furthermore, indirect seasonal budgets constructed
72 from studies of naturally fertilized systems have been capable of demonstrating an increase in
73 the strength of the biological carbon pump (Blain et al., 2007; Pollard et al., 2009), although
74 strong discrepancies in carbon to iron sequestration efficiency exist between systems. To date,
75 direct measurements of POC export from naturally fertilized blooms in the Southern Ocean
76 are limited to the Crozet Plateau (Pollard et al., 2009; Salter et al., 2012). The HNLC
77 Southern Ocean represents a region where changes in the strength of the biological pump may
78 have played a role in the glacial-interglacial CO_2 cycles (Bopp et al., 2003; Kohfeld et al.,
79 2005) and have some significance to future anthropogenic CO_2 uptake (Sarmiento and Le
80 Quéré, 1996). In this context, additional studies that directly measure POC export from
81 naturally iron-fertilized blooms in the Southern Ocean are necessary.

82 POC export can be estimated at short timescales (days to weeks) using the ^{234}Th proxy
83 (Coale and Bruland, 1985; Buesseler et al., 2006; Savoye et al., 2006), by optical imaging of
84 particles (e.g. Picheral et al., 2010) or by directly collecting particles into surface-tethered
85 sediment traps (e.g. Maiti et al., 2013 for a compilation in the Southern Ocean) or neutrally
86 buoyant sediment traps (e.g. Salter et al., 2007; Rynearson et al., 2013). Temporal variability
87 of flux in the Southern Ocean precludes extrapolation of discrete measurements to estimate
88 seasonal or annual carbon export. However seasonal export of POC can be derived from
89 biogeochemical budgets (Blain et al., 2007; Pollard et al., 2009) or be directly measured by
90 moored sediment traps (e.g. Salter et al., 2012). Biogeochemical budgets are capable of

integrating over large spatial and temporal scales but may incorporate certain assumptions and lack information about underlying mechanisms. Direct measurement by sediment traps rely on fewer assumptions but their performance is strongly related to prevailing hydrodynamic conditions (Buesseler et al., 2007a), which can be particularly problematic in the surface ocean. Measuring the hydrological conditions characterizing mooring deployments is therefore crucial to address issues surrounding the efficiency of sediment trap collection.

The ecological processes responsible for carbon export remain poorly characterized (Boyd and Trull, 2007). There is a strong requirement for quantitative analysis of the biological components of export to elucidate patterns in carbon and biomineral fluxes to the ocean interior (Francois et al., 2002; Salter et al., 2010; Henson et al., 2012; Le Moigne et al., 2012; Lima et al., 2014). Long-term deployment of moored sediment traps in areas of naturally iron fertilized production, where significant macro- and micro-nutrient gradients seasonally structure plankton communities, can help to establish links between ecological succession and carbon export. For example, sediment traps around the Crozet Plateau (Pollard et al., 2009) identified the significance of *Eucampia antarctica* var. *antarctica* resting spores for carbon transfer to the deep ocean, large empty diatom frustules for Si:C export stoichiometry (Salter et al., 2012), and heterotrophic calcifiers for the carbonate counter pump (Salter et al., 2014).

The increase in primary production resulting from natural fertilization might not necessarily lead to significant increases in carbon export. The concept of "High Biomass, Low Export" (HBLE) environments was first introduced in the Southern Ocean (Lam and Bishop, 2007). This concept is partly based on the idea that a strong grazer response to phytoplankton biomass leads to major fragmentation and remineralization of particles in the twilight zone, shallowing the remineralization horizon (Coale et al., 2004). In these environments, the efficient utilization and reprocessing of exported carbon by zooplankton leads to fecal pellet

dominated, low POC fluxes (Ebersbach et al., 2011). A synthesis of short-term sediment trap deployments, ^{234}Th estimates of upper ocean POC export and in situ primary production measurements in the Southern Ocean by Maiti et al. (2013) has highlighted the inverse relationship between primary production and export efficiency, verifying the HBLE status of many productive areas in the Southern Ocean. The iron fertilized bloom above the Kerguelen Plateau exhibits strong remineralization in the mixed layer compared to the mesopelagic, (Jacquet et al., 2008) and high bacterial carbon demand (Obernosterer et al., 2008), features consistent with a HBLE regime. Moreover, an inverse relationship between export efficiency and zooplankton biomass in the Kerguelen Plateau region support the key role of grazers in the HBLE scenario (Laurenceau et al., 2014). Efficient grazer responses to phytoplankton biomass following artificial iron fertilization of HNLC regions also demonstrate increases in net community production that are not translated to an increase in export fluxes (Lam and Bishop, 2007; Tsuda et al., 2007; Martin et al., 2013; Batten and Gower, 2014).

POC flux attenuation with depth results from processes occurring in the euphotic layer (setting the particle export efficiency, Henson et al., 2012) and processes occurring in the twilight zone between the euphotic layer and ~1000 m (Buesseler and Boyd, 2009), setting the transfer efficiency (Francois et al., 2002). These processes are mainly biologically-driven (Boyd and Trull, 2007) and involve a large diversity of ecosystem components from bacteria (Rivkin and Legendre, 2001; Giering et al., 2014), protozooplankton (Barbeau et al., 1996), mesozooplankton (Dilling and Alldredge, 2000; Smetacek et al., 2004) and mesopelagic fishes (Davison et al., 2013; Hudson et al., 2014). The net effect of these processes is summarized in a power-law formulation of POC flux attenuation with depth proposed by Martin et al. (1987) that is still commonly used in data and model applications. The b-exponent in this formulation has been reported to range from 0.4 to 1.7 (Buesseler et al., 2007b; Lampitt et al., 2008; Henson et al., 2012) in the global Ocean. Nevertheless, a change

141 in the upper mesopelagic community structure (Lam et al., 2011), and more precisely an
142 increasing contribution of mesozooplankton (Lam and Bishop, 2007; Ebersbach et al., 2011)
143 could lead to a shift toward higher POC flux attenuation with depth.

144 In this paper, we provide the first annual description of the POC and PON export
145 fluxes below the mixed layer within the naturally fertilized bloom of the Kerguelen Plateau
146 and we discuss the reliability of these measurements considering the hydrological and
147 biological context. A companion paper (Rembauville et al., 2014) addresses our final aim: to
148 identify the ecological vectors that explain the intensity and the stoichiometry of the fluxes.

149 ## 2 Material and Methods

150 ### 2.1 Trap deployment and mooring design

151 As part of the KEOPS2 multidisciplinary program, a mooring line was deployed at
152 station A3 (50°38.3 S – 72°02.6 E) in the Permanently Open Ocean Zone (POOZ), south of
153 the Polar Front (PF) (Fig. 1). The mooring line was instrumented with a Technicap PPS3
154 (0.125 m^2 collecting area, 4.75 aspect ratio) sediment trap and inclinometer (NKE S2IP) at a
155 depth of 289 m (seafloor depth 527 m) (Fig. 2). A conductivity-temperature-pressure (CTD)
156 sensor (Seabird SBE 37) and a current meter (Nortek Aquadopp) were placed on the mooring
157 line 30 m beneath the sediment trap (319 m). The sediment trap collection period started on
158 21 October 2011 until 7 September 2012. The sediment trap was composed of twelve rotating
159 sample cups (250 mL) filled with a 5 % formalin hypersaline solution buffered with sodium
160 tetraborate at pH = 8. Rotation of the carousel was programmed to sample short intervals (10-
161 14 days) between October and February, to optimize the temporal resolution of export from
162 the bloom, and long intervals (99 days) between February and September. All instruments had
163 a 1 hour recording interval. The current meter failed on the 7th April 2012.

164 ### 2.3 Surface chlorophyll data

165 The MODIS AQUA level 3 (4 km grid resolution, 8 day averages) surface chlorophyll
166 *a* product was extracted from the NASA website (http://oceancolor.gsfc.nasa.gov/) for
167 sediment trap deployment period. An annual climatology of surface chlorophyll *a*
168 concentration, based on available satellite products (1997-2013), was calculated from the
169 multisatellite Globcolour product. The Globcolour level 3, (case 1 waters, 4.63 km resolution,
170 8 day averages) product merging Seawifs, MODIS and MERIS data with GSM merging
171 model (Maritorena and Siegel, 2005) was accessed via http://www.globcolour.info. Surface
172 chlorophyll *a* concentrations derived from Globcolour (climatology) and MODIS data

173 (deployment year) were averaged across a 100 km radius centered on the sediment trap
174 deployment location (Fig. 1).

175 **2.3 Time series analyses of hydrological parameters**

176 Fast Fourier Transform (FFT) analysis was performed on the annual time series data obtained
177 from the mooring, depth and potential density anomaly (σ_θ) that were derived from the CTD
178 sensor. Significant peaks in the power spectrum were identified by comparison to red noise, a
179 theoretical signal in which the relative variance decreases with increasing frequency (Gilman
180 et al., 1963). The red noise signal was considered as a null hypothesis and its power spectrum
181 was scaled to the 99^{th} percentile of χ^2 probability. Power peaks higher than 99 % red noise
182 values were considered to be statistically significant (Schulz and Mudelsee, 2002), enabling
183 the identification of periods of major variability in time series. In order to identify the water
184 masses surrounding the trap, temperature and salinity recorded by the mooring CTD were
185 placed in context to previous CTD casts conducted at A3 during KEOPS1 (39 profiles, 23
186 January 2005 - 13 February 2005) and KEOPS2 (12 profiles, from 15 - 17 November).

187 **2.4 Sediment trap material analyses**

188 Upon recovery of the sediment trap the pH of the supernatant was measured in every cup and
189 1 mL of 37 % formalin buffered with sodium tetraborate (pH=8) was added. After allowing
190 the particulate material to settle to the base of the sample cup (~24 hrs), 60 mL of supernatant
191 was removed with a syringe and stored separately. The samples were transported in the dark
192 at 4°C (JGOFS Sediment Trap Methods, 1994) and stored under identical conditions upon
193 arrival at the laboratory until further analysis. Nitrate, nitrite, ammonium and phosphate in the
194 supernatant were analysed colorimetrically (Aminot and Kerouel, 2007) to check for possible
195 leaching of dissolved inorganic nitrogen and phosphorus from the particulate phase.

196 Samples were first transferred to a petri dish and examined under stereomicroscope
197 (Leica MZ8, x10 to x50 magnification) to determine and isolate swimmers (i.e. organisms
198 that actively entered the cup). All swimmers were carefully sorted, cleaned (rinsed with
199 preservative solution), enumerated and removed from the cups for further taxonomic
200 identification. The classification of organisms as swimmers remains subjective and there is no
201 standardized protocol. We classified zooplankton organisms as swimmers if organic material
202 and preserved structures could be observed. Empty shells, exuvia (exoskeleton remains) and
203 organic debris were considered part of the passive flux. Sample preservation prevented the
204 identification of smaller swimmers (mainly copepods) but, where possible, zooplankton were
205 identified following Boltovskoy (1999).

206 Following the removal of swimmers, samples were quantitatively split into eight
207 aliquots using a Jencons peristaltic splitter. A splitting precision of 2.9 % (coefficient of
208 variation) was determined by weighing the particulate material obtained from each of four
209 $1/8^{th}$ aliquots (see below). Aliquots for chemical analyses were centrifuged (5 min at 3000
210 rpm) with the supernatant being withdrawn after this step and replaced by milliQ-grade water
211 to remove salts (Milli-Q rinses were compared with ammonium formate. Organic carbon
212 content was not statistically different although nitrogen concentrations were significantly
213 higher, consequently Milli-Q rinses were routinely performed). The rinsing step was repeated
214 three times. The remaining pellet was freeze-dried (SGD-SERAIL, 0.05-0.1 mbar, -30 °C to
215 30 °C, 48h run) and weighed three times (Sartorius MC 210 P balance, precision 10^{-4} g) to
216 calculate the total mass. The particulate material was ground to a fine powder and used for
217 measurements of particulate constituents.

218 For particulate organic carbon (POC) and particulate organic nitrogen (PON) analyses,
219 3 to 5 mg of the freeze-dried powder was weighed directly into pre-combusted (450°C, 24h)
220 silver cups. Samples were decarbonated by adding 20 µL of 2M analytical grade Hydrochloric

221 acid (Sigma-Aldrich). Acidification was repeated until no bubbles could be seen, ensuring all
222 particulate carbonate was dissolved (Salter et al., 2010). Samples were dried overnight at 50
223 °C. POC and PON were measured with a CHN analyzer (Perkin Elmer 2400 Series II
224 CHNS/O Elemental Analyzer) calibrated with glycine. Samples were analysed in triplicate
225 with an analytical precision of less than 0.7 %. Due to the small amount of particulate
226 material in sample cups #5 and #12, replicate analyses were not possible. Uncertainty
227 propagation for POC and PON flux was calculated as the quadratic sum of errors on mass flux
228 and POC/PON content in each sample. The annual flux (± standard deviation) was calculated
229 as the sum of the time-integrated flux.

230 **3. Results**

231 **3.1 Physical conditions around trap**

232 The sediment trap was deployed in the upper layers of Upper Circumpolar Deep Water
233 (UCDW), beneath seasonally mixed Winter Water (WW) (Fig. 2). The depth of the CTD
234 sensor varied between 318 m and 322 m (1 % and 99 % quantiles), with rare deepening to 328
235 m (Fig. 3a). Variations in tilt angle of the sediment trap were also low, mostly between 1 °
236 and 5 °, and occasionally reaching 13 ° (Fig. 3d). Current speed amplitude varied between 4
237 cm s^{-1} and 23 cm s^{-1} (1 % and 99 % quantiles) with a maximum value of 33 cm s^{-1} and a mean
238 value of 9 cm s^{-1} (Fig. 3e). Horizontal flow vectors were divided between northward and
239 southward components with strongest current speeds observed to flow northward (Fig. 3f and
240 3g).

241 The range in potential temperature and salinity was 1.85–2.23 °C and 34.12 – 34.26 (1
242 % - 99 % quantiles) (Fig. 3b and 3c). From July to September 2012, a mean increase of 0.2°C
243 in potential temperature was associated with a strong diminution of high frequency noise
244 suggesting a drift of the temperature sensor. Consequently these temperature data were

245 rejected from the time-series analysis. The potential temperature/salinity diagram is compared
246 to KEOPS1 and KEOPS2 CTD downcast at station A3 (Fig. 4). The CTD sensor recorded the
247 signature of the UCDW and no intrusion of overlying WW could be detected.

248 The power spectrum of vertical sediment trap displacements identified six significant
249 peaks corresponding to frequencies of 6.2 h, 8.2 h, 23.9 h, 25.7 h and 14 days (Fig 5a).
250 Concomitant peaks of depth, angle and current speed were also observed with a period of 14
251 days. However, spectral analysis of the potential density anomaly σ_θ revealed only one
252 significant major power peak corresponding to a frequency of 12.4 h (Fig. 5b). Isopycnal
253 displacements were driven by the unique tidal component (M2, 12.4h period) and trap
254 displacements resulted from a complex combination of multiple tidal components. The power
255 spectrum analysis suggested that a 40 hour window was relevant to filter out most of the short
256 term variability (black line in Fig 3a – 3e).

257 A pseudo-lagrangian trajectory was calculated by cumulating the instantaneous current
258 vectors (Fig 6). Over short time-scales (hours to day) the trajectory displays numerous tidal
259 ellipses. The flow direction is mainly to the South-East in October 2011 to December 2012
260 and North-East from December 2011 to April 2012. For the entire current meter record (6
261 months) the overall displacement followed a 120 km northeasterly, anticlockwise trajectory
262 with an integrated current speed of approximately 1 cm s^{-1}.

263 **3.2 Seasonality of surface chlorophyll *a* concentration above trap location**

264 The seasonal variations of surface chlorophyll *a* concentration for the sediment trap
265 deployment period differed significantly from the long-term climatology (Fig 7a). The bloom
266 started at the beginning of November 2011, ten days after the start of the sediment trap
267 deployment. Maximum surface chlorophyll *a* values of 2.5 µg L^{-1} occurred on the first week
268 of November and subsequently declined rapidly to 0.2 µg L^{-1} in late December 2011. A

second increase in surface chlorophyll *a* up to 1 µg L^{-1} occurred in January 2012 and values decreased to winter levels of 0.2 µg L^{-1} in February 2012. A short-term increase of 0.8 µg L^{-1} occurred in mid-April 2012.

3.3 Swimmer abundances

No swimmers were found in cups #3 and #5 (Table 2). Total swimmer numbers were highest in winter (1544 individuals in cup #12). When normalized to cup opening time, swimmer intrusion rates were highest between mid-December 2011 and mid-February 2012 (from 26 to 55 individuals d^{-1}) and lower than 20 individuals d^{-1} for the remainder of the year. Swimmers were numerically dominated by copepods throughout the year, but elevated amphipod and pteropod abundances were observed at the end of January and February 2012 (Table 2). There was no significant correlation between mass flux, POC and PON fluxes and total swimmer number or intrusion rate (Spearman's correlation test, p >0,01). Copepods were essentially small cyclopoid species. Amphipods were predominantly represented by the hyperidean *Cyllopus magellanicus* and *Themisto gaudichaudii*. Pteropods were represented by *Clio pyramidata*, *Limacina helicina* forma *antarctica* and *Limacina retroversa* subsp. *australis*. Euphausiids were only represented by the genus *Thysanoessa*. One *Slapa thompsoni* salp (aggregate form) was found in the last winter cup #12.

3.4 Seasonal particulate organic carbon and nitrogen fluxes

Particulate organic carbon flux ranged from 0.15 to 0.55 mmol m^{-2} d^{-1} during the productive period except during two short export events of 1.6 ± 0.04 and 1.5 ± 0.04 mmol m^{-2} d^{-1} sampled in cups #4 (2 to 12 December 2011) and #9 (25 January to 8 February 2012), respectively (Fig. 7b). The two flux events occurred with an approximate time lag of one month compared to peaks in surface chlorophyll *a* values. A modest value of 0.27±0.01 mmol m^{-2} d^{-1} was observed in autumn (cup #11, 22 February to 30 May 2012). The lowest POC flux

was measured during winter (0.04 mmol m^{-2} d^{-1}, cup #12, 31 May to 7 October). Assuming that POC export was negligible from mid September to mid October, the annually integrated POC flux was 98.2 ± 4.4 mmol m^{-2} y^{-1} (Table 1). The two short (<14 days) export events accounted for 16.2±0.5 % (cup #4) and 21.0±0.6 % (cup #9) of the annual carbon export out of the mixed layer (Table 1). Mass percentage of organic carbon ranged from 3.3 % to 17.4 % (Fig. 7b). Values were slightly higher in autumn and winter (respectively 13.1±0.2 % and 11±2.1 % in cups #11 and #12) than in the summer, with the exception of cup #5 where the highest value of 17.4 % was observed. PON fluxes followed the same seasonal patterns as POC. This resulted in a relatively stable POC:PON ratio that varied between 6.1 to 7.4, except in the autumn cup #11 were it exceeded 8.1 (Table 1).

4 Discussion

4.1 Physical conditions of trap deployment

Moored sediment traps can be subject to hydrodynamic biases that affect the accuracy of particle collection (Buesseler et al., 2007a). The aspect ratio, tilt and horizontal flow regimes are important considerations when assessing sediment trap performance. Specifically, the line angle and aspect ratio of cylindrical traps can result in oversampling (Hawley, 1988). Horizontal current velocities of 12 cm s^{-1} are often invoked as a critical threshold over which particles are no longer quantitatively sampled (Baker et al., 1988). During the sediment trap deployment period we observed generally low current speeds (mean < 10 cm s^{-1}) with 75% of the recorded data lower than 12 cm s^{-1}. Despite the high aspect ratio of the PPS3 trap (4.75), and the small mooring line angle deviations, it is likely that episodic increases in current velocities (>12 cm s^{-1}) impacted collection efficiency. When integrated over the entire current meter record (October 2011 to April 2012), the resulting flow is consistent with the annual

316 northeastward, low velocity (~ 1 cm s^{-1}) geostrophic flow previously reported over the
317 central part of the Kerguelen plateau (Park et al., 2008b).

318 The depth of the winter mixed layer (WML) on the Kerguelen Plateau is usually
319 shallower than 250 m (Park et al., 1998; Metzl et al., 2006). The sediment trap deployment
320 depth of ~300 m was selected to sample particle flux exiting the WML. The moored CTD
321 sensor did not record any evidence of a winter water incursion during the deployment period,
322 confirming the WML did not reach the trap depth. The small depth variations observed during
323 the deployment period resulted from vertical displacement of the trap. Variations of σ_θ may
324 have resulted from both vertical displacement of the CTD sensor and possible isopycnal
325 displacements due to strong internal waves that can occur with an amplitude of > 50 m at this
326 depth (Park et al., 2008a). Our measurements demonstrate that isopycnal displacements are
327 consistent with the M2 (moon 2, 12.4 h period) tidal forcing described in physical modeling
328 studies (Maraldi et al., 2009, 2011). Spectral analysis indicates that high frequency tidal
329 currents are the major circulation components. Time-integrated currents suggest that
330 advection is weak and occurs over longer timescale (months). Assuming the current flow
331 measured at the sediment trap deployment depth is representative of the prevailing current
332 under the WML, more than three months are required for particles to leave the plateau from
333 the A3 station, a timescale larger than the bloom duration itself. Therefore we consider that
334 the particles collected in the sediment trap at station A3 were produced in the surface waters
335 located above the plateau during bloom conditions.

336 **4.2 Swimmers and particle solubilization**

337 Aside from the hydrodynamic effects discussed above, other potential biases characterizing
338 sediment trap deployments, particularly those in shallow waters, is the presence of swimmers
339 and particle solubilization. Swimmers can artificially increase POC fluxes by entering the

cups and releasing particulate organic matter or decrease the flux by feeding in the trap funnel (Buesseler et al., 2007a). Some studies have focused specifically on swimmer communities collected in shallow sediment traps (Matsuno et al., 2014 and references therein) although trap collection of swimmers is probably selective and therefore not quantitative. Total swimmer intrusion rate was highest in cups #6 to #9 (December 2011 to February 2012) generally through the representation of copepods and amphipods (Table 2) The maximum swimmer intrusion rate in mid-summer as well as the copepod dominance is consistent with the fourfold increase in mesozooplankton abundance observed from winter to summer (Carlotti et al., 2014). Swimmer abundance was not correlated with mass flux, POC or PON fluxes, suggesting that their presence did not systematically affect particulate fluxes inside the cups. Nevertheless such correlations cannot rule out the possibility of swimmers feeding in the trap funnel modifying particle flux collection.

Particle solubilization in preservative solutions may also lead to an underestimation of total flux measured in sediment traps. Previous analyses from traps poisoned with mercuric chloride suggest that ~30 % of total organic carbon flux can be found in the dissolved phase and much higher values of 50 % and 90 % may be observed for nitrogen and phosphorous, respectively (Antia, 2005; O'Neill et al., 2005). Unfortunately the use of a formaldehyde-based preservative in our trap samples precludes any direct estimate of excess of dissolved organic carbon in the sample cup supernatant. Furthermore, corrections for particle leaching have been considered problematic in the presence of swimmers since a fraction of the leaching may originate from the swimmers themselves (Antia, 2005), potentially leading to over-correction. Particles solubilization may have occurred in our samples as evidenced by excess PO_4^{3-} in the supernatant. However the largest values were measured in sample cups where total swimmers were abundant (cups #8 to #12, data not shown). Consequently, it was not possible to discriminate solubilisation of P from swimmers and passively settling particles

365 and it therefore remains difficult to quantify the effect of particle leaching. However, leaching
366 of POC should be less problematic in formalin-preserved samples because aldehydes fix
367 organic matter, rather than poisoning microbial activity.

368 **4.3 Seasonal dynamic of POC export**

369 The sediment trap record obtained from station A3 provides the first direct estimate of POC
370 export covering an entire season over the naturally fertilized Kerguelen Plateau. We observed
371 a temporal lag of one month between the two surface chlorophyll *a* peaks and the two export
372 events. Based on a compilation of annual sediment trap deployments Lutz et al. (2007)
373 reported that export quickly follows primary production at low latitudes whereas a time lag up
374 to two months could occur at higher latitudes. A 1-2 month lag was observed between
375 production and export in the pacific sector of the Southern Ocean (Buesseler et al., 2001), as
376 well as along 170°W (Honjo et al., 2000) and in the Australian sector of the Subantarctic
377 Zone (Rigual-Hernández et al., 2015). The temporal lag between surface production and
378 measured export in deep traps can originates from ecological processes in the upper ocean
379 (e.g. carbon retention in the mixed layer) as well as slow sinking velocities (Armstrong et al.,
380 2009) and one cannot differentiate the two processes from a single deep trap signal. A global-
381 scale modeling study suggests that the strongest temporal decoupling between production and
382 export (more than one month) occurs in areas characterized by a strong seasonal variability in
383 primary production (Henson et al., 2014). The study attributes this decoupling to differences
384 in phenology of phytoplankton and zooplankton and evokes zooplankton ejection products as
385 major contributors to fast sinking particles sedimenting post bloom.

386 On the Kerguelen Plateau there is evidence that a significant fraction of
387 phytoplankton biomass comprising the two chlorophyll peaks is remineralized by a highly
388 active heterotrophic microbial community (Obernosterer et al., 2008; Christaki et al., 2014).
389 Another fraction likely is channeled toward higher trophic levels through the intense grazing

pressure that support the observed increase in zooplankton biomass (Carlotti et al., 2008,2014). Therefore an important fraction of phytoplankton biomass increases observed by satellite may not contribute to export fluxes. Notably, the POC:PON ratio measured in our trap material is close to values reported for marine diatoms (7.3 ± 1.2, Sarthou et al., 2005), compared to the C:N ratio of zooplankton faecal pellets which is typically higher (7.3 to >15, Gerber and Gerber, 1979; Checkley and Entzeroth, 1985; Morales, 1987). Simple mass balance would therefore suggest a significant contribution of phytoplanktonic cells to the POC export, which is indeed corroborated by detailed microscopic analysis (Rembauville et al., 2014).

Although we observed increasing contribution of faecal pellet carbon post-bloom (Rembauville et al., 2014), in line with the model output of Henson et al. (2014), differences in phytoplankton and zooplankton phenology do not fully explain the seasonality of export on the Kerguelen Plateau. Considering the shallow trap depth (289 m) and typical sinking speed of 100 m d^{-1} for phyto-aggregates (Allredge and Gotschalk, 1988; Peterson et al., 2005; Trull et al., 2008a), aggregate-driven export following bloom demise would suggest a short lag of a few days between production and export peaks. The temporal lag of one month measured in the present study suggest either slow sinking rates (<5 m d^{-1}) characteristic of single phytoplanktonic cells or faster sinking particles that do not originate from the peaks of surface production. It is generally accepted that satellite detection depth is 20-50 m (Gordon and McCluney, 1975), which prevents the detection of deep phytoplanktonic biomass structures (Villareal et al., 2011). Although subsurface chlorophyll maximum located around 100 m have been observed over the Kerguelen Plateau at the end of the productive period, they have been interpreted to result from the accumulation of surface production at the base of the mixed layer rather than a subsurface productivity feature (Uitz et al., 2009). In support of this detailed taxonomic analysis of the exported material highlight diatom resting spores as major

contributors to the two export fluxes rather than a composite surface community accumulated at the base of the mixed layer. The hypothesis of a mass production of nutrient-limited resting spores post-bloom with high settling rates explains the temporal patterns of export we observed (Rembauville et al., 2014). However a better knowledge of the dynamics of factors responsible for resting spore formation by diatoms remains necessary to fully validate this hypothesis.

4.4 Rapid flux attenuation over the Kerguelen Plateau

The Kerguelen Plateau annual POC export (98.2±4.4 mmol m^{-2} y^{-1}) approaches the median global ocean POC export value comprising shallow and deep sediment traps (83 mmol m^{-2} y^{-1}, Lampitt and Antia, 1997), but is also close to values observed in HNLC areas of the POOZ (11-43 mmol m^{-2} y^{-1} at 500 m, Fischer et al., 2000). Moreover, the magnitude of annual POC export measured at ~300m on the Kerguelen Plateau is comparable to deep-ocean (>2 km) POC fluxes measured from the iron-fertilized Crozet (60 mmol m^{-2} y^{-1},Salter et al., 2012) and South Georgia blooms (180 mmol m^{-2} y^{-1}, Manno et al., 2014).

The annual POC export of ~0.1 mol m^{-2} y^{-1} at 289 m (Table 1) represents only 2% of the indirect estimate of POC export (5.1 mol m^{-2} y^{-1}) at the base of the WML (200 m) on the Kerguelen Plateau based on a seasonal DIC budget (Blain et al., 2007). On shorter time scales, the POC flux recorded in the moored sediment trap represents only a small fraction (3-8%) of the POC flux at the base of the winter mixed layer (200 m) measured by different methods during KEOPS2 (Table 3). The same conclusion is true when considering the comparison with different estimates made during KEOPS1. The diversity of the methods and the difference in the depth where the POC flux was estimated render quantitative comparisons challenging, but it appears the POC fluxes measured at 289 m with the moored sediment trap are considerably lower than some other estimates. This result indicates either extremely rapid attenuation of flux between 200 m and 300 m or major sampling bias by the sediment trap.

We note that low carbon export fluxes around 300 m have been previously reported on the Kerguelen plateau. In spring 2011, UVP derived estimates of POC export at 350 m equals 0.1 to 0.3 mmol m^{-2} d^{-1} (Table 3), a value close to our reported value of 0.15 mmol m^{-2} d^{-1}. In summer 2005, POC export at 330 m from gel trap equals 0.7 mmol m^{-2} d^{-1} (Ebersbach and Trull 2008), which is also close to our value of 1.5 mmol m^{-2} d^{-1}. Using the Jouandet et al. (2014) data at 200 m (1.9 mmol m^{-2} d^{-1}) and 350 m (0.3 mmol m^{-2} d^{-1}) and the Ebersbach and Trull (2008) data at 200 m (5.2 mmol m^{-2} d^{-1}) and 330 m (0.7 mmol m^{-2} d^{-1}) leads to Martin power law exponents values of 3.3 and 4, respectively. These values are high when compared to the range of 0.4–1.7 that was initially compiled for the global ocean (Buesseler et al., 2007b). However, there is increasing evidence in support of much higher b-values in the Southern Ocean that fall in the range 0.9-3.9 (Lam and Bishop, 2007; Henson et al., 2012; Cavan et al., 2015). Our calculations are thus consistent with emerging observations in the Southern Ocean and support a scenario of strong POC flux attenuation between 200 m and 350 m over the Kerguelen Plateau

Using the aforementioned b values (3.3 and 4) and the POC flux derived from ^{234}Th deficit at 200 m in spring (Planchon et al., 2014), we estimate POC fluxes at 289 m of 0.7 to 1.1 mmol m^{-2} d^{-1}. The flux measured in our sediment trap (0.15 mmol m^{-2} d^{-1}) data represents 14 % to 21 % of this calculated flux. Very similar percentages (21 % to 27 %) are found using the POC fluxes derived from the ^{234}Th deficit in summer (Savoye et al., 2008). Therefore we consider that the moored sediment trap collected ~15-30 % of the particle flux throughout the year. Trap-derived particle fluxes can represent 0.1 to >3 times the ^{234}Th-derived particles in shallow sediment traps (Buesseler, 1991; Buesseler et al., 1994; Coppola et al., 2002; Gustafsson et al., 2004) and this difference is largely attributed to the sum of hydrodynamic biases and swimmer activities (Buesseler, 1991), although it probably also includes the effect of post-collection particle solubilisation. In the Antarctic Peninsula, ^{234}Th derived POC export

was 20 times higher than the fluxes collected by a shallow, cylindrical, moored sediment trap at 170 m (Buesseler et al., 2010). The present deployment context is less extreme (depth of 289 m, mean current speed <10 cm s^{-1}, low tilt angle, high aspect ratio of the cylindrical PPS3 trap) but we consider that hydrodynamics (current speed higher than 12 cm s^{-1} during short tidal-driven events) and possible zooplankton feeding on the trap funnel are potential biases that may explain in part the low fluxes recorded by the moored sediment trap. Therefore the low fluxes observed likely result from a combination of collection bias (hydrodynamics and swimmers) and strong attenuation of the POC flux between the base of the WML and 300 m

Despite our conclusion that the moored sediment trap deployment was characterized by a low collection efficiency of ~15-30% with reference to ^{234}Th-derived fluxes, the numerous lines of evidence discussed above appear to converge on a scenario of rapid flux attenuation. Strong POC flux attenuation over the Kerguelen Plateau compared to the open ocean is also reported by Laurenceau et al. (2014) who associate this characteristic to a HBLE scenario and invoke the role of mesozooplankton in the carbon flux attenuation. Between October and November 2011, mesozooplankton biomass in the mixed layer doubled (Carlotti et al., 2014) and summer biomass was twofold higher still (Carlotti et al., 2008). These seasonal patterns are consistent with the maximum swimmer intrusion rate and swimmer diversity observed in summer (Table 2). It has previously been concluded that zooplankton biomass is more tightly coupled to phytoplankton biomass on the plateau compared to oceanic waters, leading to higher secondary production on the plateau (Carlotti et al., 2008, 2014). Further support linking zooplankton dynamics to HBLE environments of iron-fertilized blooms are the findings of Cavan et al. (2015) that documents lowest export ratio (exported production/primary production) in the most productive, naturally fertilized area downstream of South Georgia. Another important ecosystem feature associated to the HBLE environment of the Kerguelen Plateau, and likely shared by other island-fertilized blooms in the Southern

Ocean, is the presence of mesopelagic fishes (myctophid spawning and larvae foraging site, Koubbi et al., 1991, 2001). Mesopelagic fishes can be tightly coupled to lower trophic levels (Saba and Steinberg, 2012) and can play a significant role in carbon flux attenuation (Davison et al., 2013). Although important for carbon budgets it is a compartment often neglected due to the challenge of quantitative sampling approaches. We suggest that the HBLE scenario and large attenuation of carbon flux beneath the WML at Kerguelen may represents the transfer of carbon biomass to higher and mobile trophic groups that fuel large mammal and bird populations rather than the classical remineralization-controlled vertical attenuation characterizing open ocean environments. Although technically challenging, testing this hypothesis should be a focus for future studies in this and similar regions.

5. Conclusion

We have reported the seasonal dynamics of particulate organic carbon (POC) export under the winter mixed layer (289 m) of the naturally fertilized, productive central Kerguelen Plateau. Annual POC flux was very low (98 mmol m^{-2}) and most of it occurred during two episodic (<14 days) events exported with a 1 month lag following two surface chlorophyll *a* peaks. Analysis of the hydrological conditions and a comparison with different estimates of POC fluxes in spring and summer at the same station suggest that the sediment trap was subject to possible hydrodynamic and biological biases leading to under collection of particle flux. Nevertheless the low POC export was close to other estimates of deep (>300 m) POC export at the same station and is consistent with high attenuation coefficients reported from other methods. Taken together these data suggest that the low fluxes can be explained in part by strong flux attenuation between the winter mixed layer depth (~200 m) and the trap depth (~300 m). We invoke mesozooplankton and the activity of mesopelagic fishes as possible explanations for efficient carbon retention and/or transfer to higher trophic levels at the base of the mixed layer which results in a High Biomass, Low Export environment.

The biogenic silicon, diatoms assemblages and faecal pellet fluxes are reported in a companion paper that identifies the primary ecological vectors regulating the magnitude of POC export and seasonal patterns in BSi:POC export (Rembauville et al., 2014).

Acknowledgements

We thank the Chief Scientist Prof. Bernard Quéguiner, the Captain Bernard Lassiette and his crew during the KEOPS2 mission on the R/V Marion Dufresne II. We thank Leanne Armand and Tom Trull for their constructive comments, as well as three anonymous reviewers which helped us to improve the manuscript. This work was supported by the French Research program of INSU-CNRS LEFE-CYBER (Les enveloppes fluides et l'environnement – Cycles biogéochimiques, environnement et ressources), the French ANR (Agence Nationale de la Recherche, SIMI-6 program, ANR-10-BLAN-0614), the French CNES (Centre National d'Etudes Spatiales) and the French Polar Institute IPEV (Institut Polaire Paul-Emile Victor).

References

Allredge, A.L., Gotschalk, C., 1988. In situ settling behavior of marine snow. Limnol. Oceanogr. 33, 339–351.

Aminot, A., Kerouel, R., 2007. Dosage automatique des nutriments dans les eaux marines: méthodes en flux continu. Ifremer, Plouzané, France.

Antia, A.N., 2005. Solubilization of particles in sediment traps: revising the stoichiometry of mixed layer export. Biogeosciences 2, 189–204. doi:10.5194/bg-2-189-2005

Armstrong, R.A., Peterson, M.L., Lee, C., Wakeham, S.G., 2009. Settling velocity spectra and the ballast ratio hypothesis. Deep Sea Res. Part II Top. Stud. Oceanogr. 56, 1470–1478. doi:10.1016/j.dsr2.2008.11.032

Arrigo, K.R., Worthen, D., Schnell, A., Lizotte, M.P., 1998. Primary production in Southern Ocean waters. J. Geophys. Res. Oceans 103, 15587–15600. doi:10.1029/98JC00930

Baker, E.T., Milburn, H.B., Tennant, D.A., 1988. Field assessment of sediment trap efficiency under varying flow conditions. J. Mar. Res. 46, 573–592. doi:10.1357/002224088785113522

Barbeau, K., Moffett, J.W., Caron, D.A., Croot, P.L., Erdner, D.L., 1996. Role of protozoan grazing in relieving iron limitation of phytoplankton. Nature 380, 61–64. doi:10.1038/380061a0

Batten, S.D., Gower, J.F.R., 2014. Did the iron fertilization near Haida Gwaii in 2012 affect the pelagic lower trophic level ecosystem? J. Plankton Res. 36, 925–932. doi:10.1093/plankt/fbu049

Blain, S., Quéguiner, B., Armand, L., Belviso, S., Bombled, B., Bopp, L., Bowie, A., Brunet, C., Brussaard, C., Carlotti, F., Christaki, U., Corbière, A., Durand, I., Ebersbach, F., Fuda, J.-L., Garcia, N., Gerringa, L., Griffiths, B., Guigue, C., Guillerm, C., Jacquet, S., Jeandel, C., Laan, P., Lefèvre, D., Lo Monaco, C., Malits, A., Mosseri, J., Obernosterer, I., Park, Y.-H., Picheral, M., Pondaven, P., Remenyi, T., Sandroni, V., Sarthou, G., Savoye, N., Scouarnec, L., Souhaut, M., Thuiller, D., Timmermans, K., Trull, T., Uitz, J., van Beek, P., Veldhuis, M., Vincent, D., Viollier, E., Vong, L., Wagener, T., 2007. Effect of natural iron fertilization on carbon sequestration in the Southern Ocean. Nature 446, 1070–1074. doi:10.1038/nature05700

Blain, S., Tréguer, P., Belviso, S., Bucciarelli, E., Denis, M., Desabre, S., Fiala, M., Martin Jézéquel, V., Le Fèvre, J., Mayzaud, P., Marty, J.-C., Razouls, S., 2001. A biogeochemical study of the island mass effect in the context of the iron hypothesis: Kerguelen Islands, Southern Ocean. Deep Sea Res. Part Oceanogr. Res. Pap. 48, 163–187. doi:10.1016/S0967-0637(00)00047-9

Boltovskoy, D., 1999. South Atlantic zooplankton. Backhuys.

Bopp, L., Kohfeld, K.E., Le Quéré, C., Aumont, O., 2003. Dust impact on marine biota and atmospheric CO2 during glacial periods. Paleoceanography 18, 1046. doi:10.1029/2002PA000810

Boyd, P.W., Jickells, T., Law, C.S., Blain, S., Boyle, E.A., Buesseler, K.O., Coale, K.H., Cullen, J.J., Baar, H.J.W. de, Follows, M., Harvey, M., Lancelot, C., Levasseur, M., Owens, N.P.J., Pollard, R., Rivkin, R.B., Sarmiento, J., Schoemann, V., Smetacek, V., Takeda, S., Tsuda, A., Turner, S., Watson, A.J., 2007. Mesoscale Iron Enrichment Experiments 1993-2005: Synthesis and Future Directions. Science 315, 612–617. doi:10.1126/science.1131669

Boyd, P.W., Law, C.S., Hutchins, D.A., Abraham, E.R., Croot, P.L., Ellwood, M., Frew, R.D., Hadfield, M., Hall, J., Handy, S., Hare, C., Higgins, J., Hill, P., Hunter, K.A., LeBlanc, K., Maldonado, M.T., McKay, R.M., Mioni, C., Oliver, M., Pickmere, S., Pinkerton, M., Safi, K., Sander, S., Sanudo-Wilhelmy, S.A., Smith, M., Strzepek, R., Tovar-Sanchez, A., Wilhelm, S.W., 2005. FeCycle: Attempting an iron biogeochemical budget from a mesoscale SF6 tracer experiment in unperturbed low iron waters. Glob. Biogeochem. Cycles 19, GB4S20. doi:10.1029/2005GB002494

Boyd, P.W., Trull, T.W., 2007. Understanding the export of biogenic particles in oceanic waters: Is there consensus? Prog. Oceanogr. 72, 276–312. doi:10.1016/j.pocean.2006.10.007

Buesseler, K.O., 1991. Do upper-ocean sediment traps provide an accurate record of particle flux? Nature 353, 420–423. doi:10.1038/353420a0

Buesseler, K.O., Antia, A.N., Chen, M., Fowler, S.W., Gardner, W.D., Gustafsson, Ö., Harada, K., Michaels, A.F., Rutgers v. d. Loeff, M., Sarin, M., Steinberg, D.K., Trull, T., 2007a. An assessment of the use of sediment traps for estimating upper ocean particle fluxes. J. Mar. Res. 65, 345–416.

Buesseler, K.O., Ball, L., Andrews, J., Cochran, J.K., Hirschberg, D.J., Bacon, M.P., Fleer, A., Brzezinski, M., 2001. Upper ocean export of particulate organic carbon and biogenic silica in the Southern Ocean along 170°W. Deep Sea Res. Part II Top. Stud. Oceanogr. 48, 4275–4297. doi:10.1016/S0967-0645(01)00089-3

Buesseler, K.O., Benitez-Nelson, C.R., Moran, S.B., Burd, A., Charette, M., Cochran, J.K., Coppola, L., Fisher, N.S., Fowler, S.W., Gardner, W.D., Guo, L.D., Gustafsson, Ö., Lamborg, C., Masque, P., Miquel, J.C., Passow, U., Santschi, P.H., Savoye, N., Stewart, G., Trull, T., 2006. An assessment of particulate organic carbon to thorium-234 ratios in the ocean and their impact on the application of 234Th as a POC flux proxy. Mar. Chem., Future Applications of 234Th in Aquatic Ecosystems (FATE) 100, 213–233. doi:10.1016/j.marchem.2005.10.013

Buesseler, K.O., Boyd, P.W., 2009. Shedding light on processes that control particle export and flux attenuation in the twilight zone of the open ocean. Limnol. Oceanogr. 54, 1210–1232. doi:10.4319/lo.2009.54.4.1210

Buesseler, K.O., Lamborg, C.H., Boyd, P.W., Lam, P.J., Trull, T.W., Bidigare, R.R., Bishop, J.K.B., Casciotti, K.L., Dehairs, F., Elskens, M., Honda, M., Karl, D.M., Siegel, D.A., Silver, M.W., Steinberg, D.K., Valdes, J., Mooy, B.V., Wilson, S., 2007b. Revisiting Carbon Flux Through the Ocean's Twilight Zone. Science 316, 567–570. doi:10.1126/science.1137959

Buesseler, K.O., McDonnell, A.M.P., Schofield, O.M.E., Steinberg, D.K., Ducklow, H.W., 2010. High particle export over the continental shelf of the west Antarctic Peninsula. Geophys. Res. Lett. 37, L22606. doi:10.1029/2010GL045448

Buesseler, K.O., Michaels, A.F., Siegel, D.A., Knap, A.H., 1994. A three dimensional time-dependent approach to calibrating sediment trap fluxes. Glob. Biogeochem. Cycles 8, 179–193. doi:10.1029/94GB00207

Carlotti, F., Thibault-Botha, D., Nowaczyk, A., Lefèvre, D., 2008. Zooplankton community structure, biomass and role in carbon fluxes during the second half of a phytoplankton bloom in the eastern sector of the Kerguelen Shelf (January–February 2005). Deep Sea Res. Part II Top. Stud. Oceanogr. 55, 720–733. doi:10.1016/j.dsr2.2007.12.010

Cavan, E.L., Le Moigne, F. a. c., Poulton, A.J., Tarling, G.A., Ward, P., Daniels, C.J., Fragoso, G., Sanders, R.J., 2015. Zooplankton fecal pellets control the attenuation of particulate organic carbon flux in the Scotia Sea, Southern Ocean. Geophys. Res. Lett. 2014GL062744. doi:10.1002/2014GL062744

Checkley, D.M., Entzeroth, L.C., 1985. Elemental and isotopic fractionation of carbon and nitrogen by marine, planktonic copepods and implications to the marine nitrogen cycle. J. Plankton Res. 7, 553–568. doi:10.1093/plankt/7.4.553

Christaki, U., Lefèvre, D., Georges, C., Colombet, J., Catala, P., Courties, C., Sime-Ngando, T., Blain, S., Obernosterer, I., 2014. Microbial food web dynamics during spring phytoplankton blooms in the naturally iron-fertilized Kerguelen area (Southern Ocean). Biogeosciences 11, 6739–6753. doi:10.5194/bg-11-6739-2014

Coale, K.H., Bruland, K.W., 1985. ^{234}Th: ^{238}U Disequilibria Within the California Current. Limnol. Oceanogr. 30, 22–33.

Coale, K.H., Johnson, K.S., Chavez, F.P., Buesseler, K.O., Barber, R.T., Brzezinski, M.A., Cochlan, W.P., Millero, F.J., Falkowski, P.G., Bauer, J.E., Wanninkhof, R.H., Kudela, R.M., Altabet, M.A., Hales, B.E., Takahashi, T., Landry, M.R., Bidigare, R.R., Wang, X., Chase, Z., Strutton, P.G., Friederich, G.E., Gorbunov, M.Y., Lance, V.P., Hilting, A.K., Hiscock, M.R., Demarest, M., Hiscock, W.T., Sullivan, K.F., Tanner, S.J., Gordon, R.M., Hunter, C.N., Elrod, V.A., Fitzwater, S.E., Jones, J.L., Tozzi, S., Koblizek, M., Roberts, A.E., Herndon, J., Brewster, J., Ladizinsky, N., Smith, G., Cooper, D., Timothy, D., Brown, S.L., Selph, K.E., Sheridan, C.C., Twining, B.S., Johnson, Z.I., 2004a. Southern Ocean Iron Enrichment Experiment: Carbon Cycling in High- and Low-Si Waters. Science 304, 408–414. doi:10.1126/science.1089778

Coale, K.H., Johnson, K.S., Chavez, F.P., Buesseler, K.O., Barber, R.T., Brzezinski, M.A., Cochlan, W.P., Millero, F.J., Falkowski, P.G., Bauer, J.E., Wanninkhof, R.H., Kudela, R.M., Altabet, M.A., Hales, B.E., Takahashi, T., Landry, M.R., Bidigare, R.R., Wang, X., Chase, Z., Strutton, P.G., Friederich, G.E., Gorbunov, M.Y., Lance, V.P., Hilting, A.K., Hiscock, M.R., Demarest, M., Hiscock, W.T., Sullivan, K.F., Tanner, S.J., Gordon, R.M., Hunter, C.N., Elrod, V.A., Fitzwater, S.E., Jones, J.L., Tozzi, S., Koblizek, M., Roberts, A.E., Herndon, J., Brewster, J., Ladizinsky, N., Smith, G., Cooper, D., Timothy, D., Brown, S.L., Selph, K.E., Sheridan, C.C., Twining, B.S., Johnson, Z.I., 2004b. Southern Ocean Iron Enrichment Experiment: Carbon Cycling in High- and Low-Si Waters. Science 304, 408–414. doi:10.1126/science.1089778

Coppola, L., Roy-Barman, M., Wassmann, P., Mulsow, S., Jeandel, C., 2002. Calibration of sediment traps and particulate organic carbon export using 234Th in the Barents Sea. Mar. Chem. 80, 11–26. doi:10.1016/S0304-4203(02)00071-3

Davison, P.C., Checkley Jr., D.M., Koslow, J.A., Barlow, J., 2013. Carbon export mediated by mesopelagic fishes in the northeast Pacific Ocean. Prog. Oceanogr. 116, 14–30. doi:10.1016/j.pocean.2013.05.013

De Baar, H.J.W., Boyd, P.W., Coale, K.H., Landry, M.R., Tsuda, A., Assmy, P., Bakker, D.C.E., Bozec, Y., Barber, R.T., Brzezinski, M.A., Buesseler, K.O., Boyé, M., Croot, P.L., Gervais, F., Gorbunov, M.Y., Harrison, P.J., Hiscock, W.T., Laan, P., Lancelot, C., Law, C.S., Levasseur, M., Marchetti, A., Millero, F.J., Nishioka, J., Nojiri, Y., van Oijen, T., Riebesell, U., Rijkenberg, M.J.A., Saito, H., Takeda, S., Timmermans, K.R., Veldhuis, M.J.W., Waite, A.M., Wong, C.-S., 2005. Synthesis of iron fertilization experiments: From the Iron Age in the Age of Enlightenment. J. Geophys. Res. Oceans 110, C09S16. doi:10.1029/2004JC002601

De Baar, H.J.W., Buma, A.G.J., Nolting, R.F., Cadée, G.C., Jacques, G., Tréguer, P., 1990. On iron limitation of the Southern Ocean: experimental observations in the Weddell and Scotia Seas. Mar. Ecol. Prog. Ser. 65, 105–122. doi:doi:10.3354/meps065105

Dehairs, F., Shopova, D., Ober, S., Veth, C., Goeyens, L., 1997. Particulate barium stocks and oxygen consumption in the Southern Ocean mesopelagic water column during spring and early summer: relationship with export production. Deep Sea Res. Part II Top. Stud. Oceanogr. 44, 497–516. doi:10.1016/S0967-0645(96)00072-0

Dilling, L., Alldredge, A.L., 2000. Fragmentation of marine snow by swimming macrozooplankton: A new process impacting carbon cycling in the sea. Deep Sea Res. Part Oceanogr. Res. Pap. 47, 1227–1245. doi:10.1016/S0967-0637(99)00105-3

Dunne, J.P., Sarmiento, J.L., Gnanadesikan, A., 2007. A synthesis of global particle export from the surface ocean and cycling through the ocean interior and on the seafloor. Glob. Biogeochem. Cycles 21, GB4006. doi:10.1029/2006GB002907

Ebersbach, F., Trull, T.W., 2008. Sinking particle properties from polyacrylamide gels during the KErguelen Ocean and Plateau compared Study (KEOPS): Zooplankton control of carbon export in an area of persistent natural iron inputs in the Southern Ocean. Limnol. Oceanogr. 53, 212–224. doi:10.4319/lo.2008.53.1.0212

Ebersbach, F., Trull, T.W., Davies, D.M., Bray, S.G., 2011. Controls on mesopelagic particle fluxes in the Sub-Antarctic and Polar Frontal Zones in the Southern Ocean south of Australia in summer—Perspectives from free-drifting sediment traps. Deep Sea Res. Part II Top. Stud. Oceanogr. 58, 2260–2276. doi:10.1016/j.dsr2.2011.05.025

Fischer, G., Ratmeyer, V., Wefer, G., 2000. Organic carbon fluxes in the Atlantic and the Southern Ocean: relationship to primary production compiled from satellite radiometer data. Deep Sea Res. Part II Top. Stud. Oceanogr. 47, 1961–1997. doi:10.1016/S0967-0645(00)00013-8

Francois, R., Honjo, S., Krishfield, R., Manganini, S., 2002. Factors controlling the flux of organic carbon to the bathypelagic zone of the ocean. Glob. Biogeochem. Cycles 16, 1087. doi:10.1029/2001GB001722

Gall, M.P., Strzepek, R., Maldonado, M., Boyd, P.W., 2001. Phytoplankton processes. Part 2: Rates of primary production and factors controlling algal growth during the Southern Ocean Iron RElease Experiment (SOIREE). Deep Sea Res. Part II Top. Stud. Oceanogr., The Southern Ocean Iron Release Experiment (SOIREE) 48, 2571–2590. doi:10.1016/S0967-0645(01)00009-1

Gehlen, M., Bopp, L., Emprin, N., Aumont, O., Heinze, C., Ragueneau, O., 2006. Reconciling surface ocean productivity, export fluxes and sediment composition in a global biogeochemical ocean model. Biogeosciences 3, 521–537. doi:10.5194/bg-3-521-2006

Gerber, R.P., Gerber, M.B., 1979. Ingestion of natural particulate organic matter and subsequent assimilation, respiration and growth by tropical lagoon zooplankton. Mar. Biol. 52, 33–43. doi:10.1007/BF00386855

Giering, S.L.C., Sanders, R., Lampitt, R.S., Anderson, T.R., Tamburini, C., Boutrif, M., Zubkov, M.V., Marsay, C.M., Henson, S.A., Saw, K., Cook, K., Mayor, D.J., 2014. Reconciliation of the carbon budget in the ocean/'s twilight zone. Nature 507, 480–483. doi:10.1038/nature13123

Gilman, D.L., Fuglister, F.J., Mitchell, J.M., 1963. On the Power Spectrum of "Red Noise." J. Atmospheric Sci. 20, 182–184. doi:10.1175/1520-0469(1963)020<0182:OTPSON>2.0.CO;2

Gonzalez, H.E., Smetacek, V., 1994. The possible role of the cyclopoid copepod Oithona in retarding vertical flux of zooplankton faecal material. Mar. Ecol.-Prog. Ser. 113, 233–246.

Gordon, H.R., McCluney, W.R., 1975. Estimation of the depth of sunlight penetration in the sea for remote sensing. Appl. Opt. 14, 413–416.

Gruber, N., Gloor, M., Mikaloff Fletcher, S.E., Doney, S.C., Dutkiewicz, S., Follows, M.J., Gerber, M., Jacobson, A.R., Joos, F., Lindsay, K., Menemenlis, D., Mouchet, A., Müller, S.A., Sarmiento, J.L., Takahashi, T., 2009. Oceanic sources, sinks, and transport of atmospheric CO2. Glob. Biogeochem. Cycles 23, GB1005. doi:10.1029/2008GB003349

Gustafsson, O., Andersson, P., Roos, P., Kukulska, Z., Broman, D., Larsson, U., Hajdu, S., Ingri, J., 2004. Evaluation of the collection efficiency of upper ocean sub-photic-layer sediment traps: A 24-month in situ calibration in the open Baltic Sea using 234Th. Limnol. Oceanogr. Methods 2, 62–74. doi:10.4319/lom.2004.2.62

Hawley, N., 1988. Flow in Cylindrical Sediment Traps. J. Gt. Lakes Res. 14, 76–88. doi:10.1016/S0380-1330(88)71534-8

Henson, S.A., Sanders, R., Madsen, E., 2012. Global patterns in efficiency of particulate organic carbon export and transfer to the deep ocean. Glob. Biogeochem. Cycles 26, GB1028. doi:10.1029/2011GB004099

Henson, S.A., Sanders, R., Madsen, E., Morris, P.J., Le Moigne, F., Quartly, G.D., 2011. A reduced estimate of the strength of the ocean's biological carbon pump. Geophys. Res. Lett. 38, L04606. doi:10.1029/2011GL046735

Henson, S.A., Yool, A., Sanders, R., 2014. Variability in efficiency of particulate organic carbon export: A model study. Glob. Biogeochem. Cycles 29, GB4965. doi:10.1002/2014GB004965
Hiscock, W.T., Millero, F.J., 2005. Nutrient and carbon parameters during the Southern Ocean iron experiment (SOFeX). Deep Sea Res. Part Oceanogr. Res. Pap. 52, 2086–2108. doi:10.1016/j.dsr.2005.06.010
Honda, M.C., Kawakami, H., Sasaoka, K., Watanabe, S., Dickey, T., 2006. Quick transport of primary produced organic carbon to the ocean interior. Geophys. Res. Lett. 33, L16603. doi:10.1029/2006GL026466
Honjo, S., Francois, R., Manganini, S., Dymond, J., Collier, R., 2000. Particle fluxes to the interior of the Southern Ocean in the Western Pacific sector along 170°W. Deep Sea Res. Part II Top. Stud. Oceanogr. 47, 3521–3548. doi:10.1016/S0967-0645(00)00077-1
Honjo, S., Manganini, S.J., Krishfield, R.A., Francois, R., 2008. Particulate organic carbon fluxes to the ocean interior and factors controlling the biological pump: A synthesis of global sediment trap programs since 1983. Prog. Oceanogr. 76, 217–285. doi:10.1016/j.pocean.2007.11.003
Hudson, J.M., Steinberg, D.K., Sutton, T.T., Graves, J.E., Latour, R.J., 2014. Myctophid feeding ecology and carbon transport along the northern Mid-Atlantic Ridge. Deep Sea Res. Part Oceanogr. Res. Pap. 93, 104–116. doi:10.1016/j.dsr.2014.07.002
Jacquet, S.H.M., Dehairs, F., Savoye, N., Obernosterer, I., Christaki, U., Monnin, C., Cardinal, D., 2008. Mesopelagic organic carbon remineralization in the Kerguelen Plateau region tracked by biogenic particulate Ba. Deep Sea Res. Part II Top. Stud. Oceanogr. 55, 868–879. doi:10.1016/j.dsr2.2007.12.038
JGOFS Sediment Trap Methods, 1994. , in: Protocols for the Joint Global Ocean Flux Study (JGOFS) Core Measurements. Intergovernmental Oceanographic Commission, Scientific Committee on Oceanic Research Manual and Guides, UNESCO, pp. 157–164.
Jouandet, M.P., Blain, S., Metzl, N., Brunet, C., Trull, T.W., Obernosterer, I., 2008. A seasonal carbon budget for a naturally iron-fertilized bloom over the Kerguelen Plateau in the Southern Ocean. Deep Sea Res. Part II Top. Stud. Oceanogr., KEOPS: Kerguelen Ocean and Plateau compared Study 55, 856–867. doi:10.1016/j.dsr2.2007.12.037
Jouandet, M.-P., Jackson, G.A., Carlotti, F., Picheral, M., Stemmann, L., Blain, S., 2014. Rapid formation of large aggregates during the spring bloom of Kerguelen Island: observations and model comparisons. Biogeosciences 11, 4393–4406. doi:10.5194/bg-11-4393-2014
Jouandet, M.-P., Trull, T.W., Guidi, L., Picheral, M., Ebersbach, F., Stemmann, L., Blain, S., 2011. Optical imaging of mesopelagic particles indicates deep carbon flux beneath a natural iron-fertilized bloom in the Southern Ocean. Limnol. Oceanogr. 56, 1130–1140. doi:10.4319/lo.2011.56.3.1130
Karleskind, P., Lévy, M., Memery, L., 2011. Subduction of carbon, nitrogen, and oxygen in the northeast Atlantic. J. Geophys. Res. Oceans 116, C02025. doi:10.1029/2010JC006446
Kohfeld, K.E., Quéré, C.L., Harrison, S.P., Anderson, R.F., 2005. Role of Marine Biology in Glacial-Interglacial CO2 Cycles. Science 308, 74–78. doi:10.1126/science.1105375
Korb, R.E., Whitehouse, M., 2004. Contrasting primary production regimes around South Georgia, Southern Ocean: large blooms versus high nutrient, low chlorophyll waters. Deep Sea Res. Part Oceanogr. Res. Pap. 51, 721–738. doi:10.1016/j.dsr.2004.02.006
Koubbi, P., Duhamel, G., Hebert, C., 2001. Seasonal relative abundance of fish larvae inshore at Îles Kerguelen, Southern Ocean. Antarct. Sci. 13, 385–392. doi:10.1017/S0954102001000542
Koubbi, P., Ibanez, F., Duhamel, G., 1991. Environmental influences on spatio-temporal oceanic distribution of ichthyoplankton around the Kerguelen Islands (Southern Ocean). Mar. Ecol. Prog. Ser. 72, 225–238.
Lampitt, R.S., Antia, A.N., 1997. Particle flux in deep seas: regional characteristics and temporal variability. Deep Sea Res. Part Oceanogr. Res. Pap. 44, 1377–1403. doi:10.1016/S0967-0637(97)00020-4
Lampitt, R.S., Boorman, B., Brown, L., Lucas, M., Salter, I., Sanders, R., Saw, K., Seeyave, S., Thomalla, S.J., Turnewitsch, R., 2008. Particle export from the euphotic zone: Estimates using a novel drifting sediment trap, 234Th and new production. Deep Sea Res. Part Oceanogr. Res. Pap. 55, 1484–1502. doi:10.1016/j.dsr.2008.07.002
Lam, P.J., Bishop, J.K.B., 2007. High biomass, low export regimes in the Southern Ocean. Deep Sea Res. Part II Top. Stud. Oceanogr. 54, 601–638. doi:10.1016/j.dsr2.2007.01.013
Lam, P.J., Doney, S.C., Bishop, J.K.B., 2011. The dynamic ocean biological pump: Insights from a global compilation of particulate organic carbon, CaCO3, and opal concentration profiles from the mesopelagic. Glob. Biogeochem. Cycles 25, GB3009. doi:10.1029/2010GB003868
Landry, M.R., Constantinou, J., Latasa, M., Brown, S.L., Bidigare, R.R., Ondrusek, M.E., 2000. Biological response to iron fertilization in the eastern equatorial Pacific (IronEx II). III. Dynamics of phytoplankton growth and microzooplankton grazing. Mar. Ecol. Prog. Ser. 201, 57–72. doi:10.3354/meps201057
Lasbleiz, M., Leblanc, K., Blain, S., Ras, J., Cornet-Barthaux, V., Hélias Nunige, S., Quéguiner, B., 2014. Pigments, elemental composition (C, N, P, and Si), and stoichiometry of particulate matter in the

763 naturally iron fertilized region of Kerguelen in the Southern Ocean. Biogeosciences 11, 5931–5955.
764 doi:10.5194/bg-11-5931-2014
765 Laurenceau, E.C., Trull, T.W., Davies, D.M., Bray, S.G., Doran, J., Planchon, F., Carlotti, F., Jouandet, M.-P.,
766 Cavagna, A.-J., Waite, A.M., Blain, S., 2014. The relative importance of phytoplankton aggregates and
767 zooplankton fecal pellets to carbon export: insights from free-drifting sediment trap deployments in
768 naturally iron-fertilised waters near the Kerguelen plateau. Biogeosciences Discuss 11, 13623–13673.
769 doi:10.5194/bgd-11-13623-2014
770 Laws, E.A., D'Sa, E., Naik, P., 2011. Simple equations to estimate ratios of new or export production to total
771 production from satellite-derived estimates of sea surface temperature and primary production. Limnol.
772 Oceanogr. Methods 593–601. doi:10.4319/lom.2011.9.593
773 Laws, E.A., Falkowski, P.G., Smith, W.O., Ducklow, H., McCarthy, J.J., 2000. Temperature effects on export
774 production in the open ocean. Glob. Biogeochem. Cycles 14, 1231–1246. doi:10.1029/1999GB001229
775 Lefèvre, D., Guigue, C., Obernosterer, I., 2008. The metabolic balance at two contrasting sites in the Southern
776 Ocean: The iron-fertilized Kerguelen area and HNLC waters. Deep Sea Res. Part II Top. Stud.
777 Oceanogr., KEOPS: Kerguelen Ocean and Plateau compared Study 55, 766–776.
778 doi:10.1016/j.dsr2.2007.12.006
779 Le Moigne, F.A.C., Sanders, R.J., Villa-Alfageme, M., Martin, A.P., Pabortsava, K., Planquette, H., Morris, P.J.,
780 Thomalla, S.J., 2012. On the proportion of ballast versus non-ballast associated carbon export in the
781 surface ocean. Geophys. Res. Lett. 39, L15610. doi:10.1029/2012GL052980
782 Lenton, A., Tilbrook, B., Law, R.M., Bakker, D., Doney, S.C., Gruber, N., Ishii, M., Hoppema, M., Lovenduski,
783 N.S., Matear, R.J., McNeil, B.I., Metzl, N., Mikaloff Fletcher, S.E., Monteiro, P.M.S., Rödenbeck, C.,
784 Sweeney, C., Takahashi, T., 2013. Sea–air CO2 fluxes in the Southern Ocean for the period 1990–2009.
785 Biogeosciences 10, 4037–4054. doi:10.5194/bg-10-4037-2013
786 Le Quéré, C., Andres, R.J., Boden, T., Conway, T., Houghton, R.A., House, J.I., Marland, G., Peters, G.P., van
787 der Werf, G.R., Ahlström, A., Andrew, R.M., Bopp, L., Canadell, J.G., Ciais, P., Doney, S.C., Enright,
788 C., Friedlingstein, P., Huntingford, C., Jain, A.K., Jourdain, C., Kato, E., Keeling, R.F., Klein
789 Goldewijk, K., Levis, S., Levy, P., Lomas, M., Poulter, B., Raupach, M.R., Schwinger, J., Sitch, S.,
790 Stocker, B.D., Viovy, N., Zaehle, S., Zeng, N., 2013. The global carbon budget 1959–2011. Earth Syst.
791 Sci. Data 5, 165–185. doi:10.5194/essd-5-165-2013
792 Levy, M., Bopp, L., Karleskind, P., Resplandy, L., Ethe, C., Pinsard, F., 2013. Physical pathways for carbon
793 transfers between the surface mixed layer and the ocean interior. Glob. Biogeochem. Cycles 27, 1001–
794 1012. doi:10.1002/gbc.20092
795 Lima, I.D., Lam, P.J., Doney, S.C., 2014a. Dynamics of particulate organic carbon flux in a global ocean model.
796 Biogeosciences 11, 1177–1198. doi:10.5194/bg-11-1177-2014
797 Lima, I.D., Lam, P.J., Doney, S.C., 2014b. Dynamics of particulate organic carbon flux in a global ocean model.
798 Biogeosciences 11, 1177–1198. doi:10.5194/bg-11-1177-2014
799 Lutz, M.J., Caldeira, K., Dunbar, R.B., Behrenfeld, M.J., 2007. Seasonal rhythms of net primary production and
800 particulate organic carbon flux to depth describe the efficiency of biological pump in the global ocean.
801 J. Geophys. Res. Oceans 112, C10011. doi:10.1029/2006JC003706
802 Maiti, K., Charette, M.A., Buesseler, K.O., Kahru, M., 2013. An inverse relationship between production and
803 export efficiency in the Southern Ocean. Geophys. Res. Lett. 40, 1557–1561. doi:10.1002/grl.50219
804 Manno, C., Stowasser, G., Enderlein, P., Fielding, S., Tarling, G.A., 2014. The contribution of zooplankton
805 faecal pellets to deep carbon transport in the Scotia Sea (Southern Ocean). Biogeosciences Discuss 11,
806 16105–16134. doi:10.5194/bgd-11-16105-2014
807 Maraldi, C., Lyard, F., Testut, L., Coleman, R., 2011. Energetics of internal tides around the Kerguelen Plateau
808 from modeling and altimetry. J. Geophys. Res. Oceans 116, C06004. doi:10.1029/2010JC006515
809 Maraldi, C., Mongin, M., Coleman, R., Testut, L., 2009. The influence of lateral mixing on a phytoplankton
810 bloom: Distribution in the Kerguelen Plateau region. Deep Sea Res. Part Oceanogr. Res. Pap. 56, 963–
811 973. doi:10.1016/j.dsr.2008.12.018
812 Maritorena, S., Siegel, D.A., 2005. Consistent merging of satellite ocean color data sets using a bio-optical
813 model. Remote Sens. Environ. 94, 429–440. doi:10.1016/j.rse.2004.08.014
814 Martin, J.H., Knauer, G.A., Karl, D.M., Broenkow, W.W., 1987. VERTEX: carbon cycling in the northeast
815 Pacific. Deep Sea Res. Part Oceanogr. Res. Pap. 34, 267–285. doi:10.1016/0198-0149(87)90086-0
816 Martin, P., van der Loeff, M.R., Cassar, N., Vandromme, P., d' Ovidio, F., Stemmann, L., Rengarajan, R.,
817 Soares, M., González, H.E., Ebersbach, F., Lampitt, R.S., Sanders, R., Barnett, B.A., Smetacek, V.,
818 Naqvi, S.W.A., 2013. Iron fertilization enhanced net community production but not downward particle
819 flux during the Southern Ocean iron fertilization experiment LOHAFEX. Glob. Biogeochem. Cycles
820 27, 871–881. doi:10.1002/gbc.20077
821 Matsuno, K., Yamaguchi, A., Fujiwara, A., Onodera, J., Watanabe, E., Imai, I., Chiba, S., Harada, N., Kikuchi,
822 T., 2014. Seasonal changes in mesozooplankton swimmers collected by sediment trap moored at a

single station on the Northwind Abyssal Plain in the western Arctic Ocean. J. Plankton Res. 36, 490–502. doi:10.1093/plankt/fbt092

McLeod, D.J., Hosie, G.W., Kitchener, J.A., Takahashi, K.T., Hunt, B.P.V., 2010. Zooplankton Atlas of the Southern Ocean: The SCAR SO-CPR Survey (1991–2008). Polar Sci., Antarctic Biology in the 21st Century - Advances in and beyond IPY 4, 353–385. doi:10.1016/j.polar.2010.03.004

Measures, C.I., Brown, M.T., Selph, K.E., Apprill, A., Zhou, M., Hatta, M., Hiscock, W.T., 2013. The influence of shelf processes in delivering dissolved iron to the HNLC waters of the Drake Passage, Antarctica. Deep Sea Res. Part II Top. Stud. Oceanogr. 90, 77–88. doi:10.1016/j.dsr2.2012.11.004

Metzl, N., Brunet, C., Jabaud-Jan, A., Poisson, A., Schauer, B., 2006. Summer and winter air–sea CO2 fluxes in the Southern Ocean. Deep Sea Res. Part Oceanogr. Res. Pap. 53, 1548–1563. doi:10.1016/j.dsr.2006.07.006

Moore, J.K., Doney, S.C., Lindsay, K., 2004. Upper ocean ecosystem dynamics and iron cycling in a global three-dimensional model. Glob. Biogeochem. Cycles 18, GB4028. doi:10.1029/2004GB002220

Morales, C.E., 1987. Carbon and nitrogen content of copepod faecal pellets: effect of food concentration and feeding behaviour. Mar. Ecol. Prog. Ser. 36, 107–114.

Obernosterer, I., Christaki, U., Lefèvre, D., Catala, P., Van Wambeke, F., Lebaron, P., 2008. Rapid bacterial mineralization of organic carbon produced during a phytoplankton bloom induced by natural iron fertilization in the Southern Ocean. Deep Sea Res. Part II Top. Stud. Oceanogr. 55, 777–789. doi:10.1016/j.dsr2.2007.12.005

O'Neill, L.P., Benitez-Nelson, C.R., Styles, R.M., Tappa, E., Thunell, R.C., 2005. Diagenetic effects on particulate phosphorus samples collected using formalin poisoned sediment traps. Limnol. Oceanogr. Methods 3, 308–317. doi:10.4319/lom.2005.3.308

Park, Y.-H., Charriaud, E., Pino, D.R., Jeandel, C., 1998. Seasonal and interannual variability of the mixed layer properties and steric height at station KERFIX, southwest of Kerguelen. J. Mar. Syst. 17, 571–586. doi:10.1016/S0924-7963(98)00065-7

Park, Y.-H., Fuda, J.-L., Durand, I., Naveira Garabato, A.C., 2008a. Internal tides and vertical mixing over the Kerguelen Plateau. Deep Sea Res. Part II Top. Stud. Oceanogr. 55, 582–593. doi:10.1016/j.dsr2.2007.12.027

Park, Y.-H., Roquet, F., Durand, I., Fuda, J.-L., 2008b. Large-scale circulation over and around the Northern Kerguelen Plateau. Deep Sea Res. Part II Top. Stud. Oceanogr. 55, 566–581. doi:10.1016/j.dsr2.2007.12.030

Peterson, M.L., Wakeham, S.G., Lee, C., Askea, M.A., Miquel, J.C., 2005. Novel techniques for collection of sinking particles in the ocean and determining their settling rates. Limnol. Oceanogr. Methods 3, 520–532. doi:10.4319/lom.2005.3.520

Picheral, M., Guidi, L., Stemmann, L., Karl, D.M., Iddaoud, G., Gorsky, G., 2010. The Underwater Vision Profiler 5: An advanced instrument for high spatial resolution studies of particle size spectra and zooplankton. Limnol. Oceanogr. Methods 8, 462–473. doi:10.4319/lom.2010.8.462

Pinkerton, M.H., Smith, A.N.H., Raymond, B., Hosie, G.W., Sharp, B., Leathwick, J.R., Bradford-Grieve, J.M., 2010. Spatial and seasonal distribution of adult Oithona similis in the Southern Ocean: Predictions using boosted regression trees. Deep Sea Res. Part Oceanogr. Res. Pap. 57, 469–485. doi:10.1016/j.dsr.2009.12.010

Planchon, F., Ballas, D., Cavagna, A.-J., Bowie, A.R., Davies, D., Trull, T., Laurenceau, E., Van Der Merwe, P., Dehairs, F., 2014. Carbon export in the naturally iron-fertilized Kerguelen area of the Southern Ocean based on the 234Th approach. Biogeosciences Discuss 11, 15991–16032. doi:10.5194/bgd-11-15991-2014

Pollard, R., Sanders, R., Lucas, M., Statham, P., 2007. The Crozet Natural Iron Bloom and Export Experiment (CROZEX). Deep Sea Res. Part II Top. Stud. Oceanogr. 54, 1905–1914. doi:10.1016/j.dsr2.2007.07.023

Pollard, R.T., Salter, I., Sanders, R.J., Lucas, M.I., Moore, C.M., Mills, R.A., Statham, P.J., Allen, J.T., Baker, A.R., Bakker, D.C.E., Charette, M.A., Fielding, S., Fones, G.R., French, M., Hickman, A.E., Holland, R.J., Hughes, J.A., Jickells, T.D., Lampitt, R.S., Morris, P.J., Nédélec, F.H., Nielsdóttir, M., Planquette, H., Popova, E.E., Poulton, A.J., Read, J.F., Seeyave, S., Smith, T., Stinchcombe, M., Taylor, S., Thomalla, S., Venables, H.J., Williamson, R., Zubkov, M.V., 2009. Southern Ocean deep-water carbon export enhanced by natural iron fertilization. Nature 457, 577–580. doi:10.1038/nature07716

Redfield, A., 1934. On the proportions of organic derivatives in sea water and their relation to the composition of plankton. James Johnstone Meml. Vol. Univ. Press Liverp. 177– 192.

Rembauville, M., Blain, S., Armand, L., Quéguiner, B., Salter, I., 2014. Export fluxes in a naturally fertilized area of the Southern Ocean, the Kerguelen Plateau: ecological vectors of carbon and biogenic silica to depth (Part 2). Biogeosciences Discuss 11, 17089–17150. doi:10.5194/bgd-11-17089-2014

882 Rigual-Hernández, A.S., Trull, T.W., Bray, S.G., Closset, I., Armand, L.K., 2015. Seasonal dynamics in diatom
883 and particulate export fluxes to the deep sea in the Australian sector of the southern Antarctic Zone. J.
884 Mar. Syst. 142, 62–74. doi:10.1016/j.jmarsys.2014.10.002
885 Rivkin, R.B., Legendre, L., 2001. Biogenic carbon cycling in the upper ocean: effects of microbial respiration.
886 Science 291, 2398–2400. doi:10.1126/science.291.5512.2398
887 Rynearson, T.A., Richardson, K., Lampitt, R.S., Sieracki, M.E., Poulton, A.J., Lyngsgaard, M.M., Perry, M.J.,
888 2013. Major contribution of diatom resting spores to vertical flux in the sub-polar North Atlantic. Deep
889 Sea Res. Part Oceanogr. Res. Pap. 82, 60–71. doi:10.1016/j.dsr.2013.07.013
890 Saba, G.K., Steinberg, D.K., 2012. Abundance, Composition, and Sinking Rates of Fish Fecal Pellets in the
891 Santa Barbara Channel. Sci. Rep. 2. doi:10.1038/srep00716
892 Salter, I., Kemp, A.E.S., Lampitt, R.S., Gledhill, M., 2010. The association between biogenic and inorganic
893 minerals and the amino acid composition of settling particles. Limnol. Oceanogr. 55, 2207–2218.
894 doi:10.4319/lo.2010.55.5.2207
895 Salter, I., Kemp, A.E.S., Moore, C.M., Lampitt, R.S., Wolff, G.A., Holtvoeth, J., 2012. Diatom resting spore
896 ecology drives enhanced carbon export from a naturally iron-fertilized bloom in the Southern Ocean.
897 Glob. Biogeochem. Cycles 26, GB1014. doi:10.1029/2010GB003977
898 Salter, I., Lampitt, R.S., Sanders, R., Poulton, A., Kemp, A.E.S., Boorman, B., Saw, K., Pearce, R., 2007.
899 Estimating carbon, silica and diatom export from a naturally fertilised phytoplankton bloom in the
900 Southern Ocean using PELAGRA: A novel drifting sediment trap. Deep Sea Res. Part II Top. Stud.
901 Oceanogr., The Crozet Natural Iron Bloom and Export Experiment CROZEX 54, 2233–2259.
902 doi:10.1016/j.dsr2.2007.06.008
903 Salter, I., Schiebel, R., Ziveri, P., Movellan, A., Lampitt, R., Wolff, G.A., 2014. Carbonate counter pump
904 stimulated by natural iron fertilization in the Polar Frontal Zone. Nat. Geosci. 7, 885–889.
905 doi:10.1038/ngeo2285
906 Sarmiento, J.L., Gruber, N., 2006. Ocean Biogeochemical Dynamics. Princeton University Press, Princeton.
907 Sarmiento, J.L., Le Quéré, C., 1996. Oceanic Carbon Dioxide Uptake in a Model of Century-Scale Global
908 Warming. Science 274, 1346–1350.
909 Sarthou, G., Timmermans, K.R., Blain, S., Tréguer, P., 2005. Growth physiology and fate of diatoms in the
910 ocean: a review. J. Sea Res., Iron Resources and Oceanic Nutrients - Advancement of Global
911 Environmental Simulations 53, 25–42. doi:10.1016/j.seares.2004.01.007
912 Savoye, N., Benitez-Nelson, C., Burd, A.B., Cochran, J.K., Charette, M., Buesseler, K.O., Jackson, G.A., Roy-
913 Barman, M., Schmidt, S., Elskens, M., 2006. 234Th sorption and export models in the water column: A
914 review. Mar. Chem., Future Applications of 234Th in Aquatic Ecosystems (FATE) 100, 234–249.
915 doi:10.1016/j.marchem.2005.10.014
916 Savoye, N., Trull, T.W., Jacquet, S.H.M., Navez, J., Dehairs, F., 2008. 234Th-based export fluxes during a
917 natural iron fertilization experiment in the Southern Ocean (KEOPS). Deep Sea Res. Part II Top. Stud.
918 Oceanogr., KEOPS: Kerguelen Ocean and Plateau compared Study 55, 841–855.
919 doi:10.1016/j.dsr2.2007.12.036
920 Schlitzer, R., 2004. Export production in the Equatorial and North Pacific derived from dissolved oxygen,
921 nutrient and carbon data. J. Oceanogr. Vol 60 No 1 Pp 53–62.
922 Schulz, M., Mudelsee, M., 2002. REDFIT: estimating red-noise spectra directly from unevenly spaced
923 paleoclimatic time series. Comput. Geosci. 28, 421–426. doi:10.1016/S0098-3004(01)00044-9
924 Seeyave, S., Lucas, M.I., Moore, C.M., Poulton, A.J., 2007. Phytoplankton productivity and community
925 structure in the vicinity of the Crozet Plateau during austral summer 2004/2005. Deep Sea Res. Part II
926 Top. Stud. Oceanogr., The Crozet Natural Iron Bloom and Export Experiment CROZEX 54, 2020–
927 2044. doi:10.1016/j.dsr2.2007.06.010
928 Smetacek, V., Assmy, P., Henjes, J., 2004. The role of grazing in structuring Southern Ocean pelagic ecosystems
929 and biogeochemical cycles. Antarct. Sci. 16, 541–558. doi:10.1017/S0954102004002317
930 Tarling, G.A., Ward, P., Atkinson, A., Collins, M.A., Murphy, E.J., 2012. DISCOVERY 2010: Spatial and
931 temporal variability in a dynamic polar ecosystem. Deep Sea Res. Part II Top. Stud. Oceanogr. 59–60,
932 1–13. doi:10.1016/j.dsr2.2011.10.001
933 Thomalla, S.J., Fauchereau, N., Swart, S., Monteiro, P.M.S., 2011. Regional scale characteristics of the seasonal
934 cycle of chlorophyll in the Southern Ocean. Biogeosciences 8, 2849–2866. doi:10.5194/bg-8-2849-
935 2011
936 Trull, T.W., Bray, S.G., Buesseler, K.O., Lamborg, C.H., Manganini, S., Moy, C., Valdes, J., 2008. In situ
937 measurement of mesopelagic particle sinking rates and the control of carbon transfer to the ocean
938 interior during the Vertical Flux in the Global Ocean (VERTIGO) voyages in the North Pacific. Deep
939 Sea Res. Part II Top. Stud. Oceanogr. 55, 1684–1695. doi:10.1016/j.dsr2.2008.04.021

Trull, T.W., Davies, D., Casciotti, K., 2008. Insights into nutrient assimilation and export in naturally iron-fertilized waters of the Southern Ocean from nitrogen, carbon and oxygen isotopes. Deep Sea Res. Part II Top. Stud. Oceanogr. 55, 820–840. doi:10.1016/j.dsr2.2007.12.035

Tsuda, A., Takeda, S., Saito, H., Nishioka, J., Kudo, I., Nojiri, Y., Suzuki, K., Uematsu, M., Wells, M.L., Tsumune, D., Yoshimura, T., Aono, T., Aramaki, T., Cochlan, W.P., Hayakawa, M., Imai, K., Isada, T., Iwamoto, Y., Johnson, W.K., Kameyama, S., Kato, S., Kiyosawa, H., Kondo, Y., Levasseur, M., Machida, R.J., Nagao, I., Nakagawa, F., Nakanishi, T., Nakatsuka, S., Narita, A., Noiri, Y., Obata, H., Ogawa, H., Oguma, K., Ono, T., Sakuragi, T., Sasakawa, M., Sato, M., Shimamoto, A., Takata, H., Trick, C.G., Watanabe, Y.W., Wong, C.S., Yoshie, N., 2007. Evidence for the grazing hypothesis: Grazing reduces phytoplankton responses of the HNLC ecosystem to iron enrichment in the western subarctic pacific (SEEDS II). J. Oceanogr. 63, 983–994. doi:10.1007/s10872-007-0082-x

Turner, J.T., 2002. Zooplankton fecal pellets, marine snow and sinking phytoplankton blooms. Aquat. Microb. Ecol. 27, 57–102. doi:10.3354/ame027057

Uitz, J., Claustre, H., Griffiths, F.B., Ras, J., Garcia, N., Sandroni, V., 2009. A phytoplankton class-specific primary production model applied to the Kerguelen Islands region (Southern Ocean). Deep Sea Res. Part Oceanogr. Res. Pap. 56, 541–560. doi:10.1016/j.dsr.2008.11.006

Villareal, T.A., Adornato, L., Wilson, C., Schoenbaechler, C.A., 2011. Summer blooms of diatom-diazotroph assemblages and surface chlorophyll in the North Pacific gyre: A disconnect. J. Geophys. Res. Oceans 116, C03001. doi:10.1029/2010JC006268

Volk, T., Hoffert, M.I., 1985. Ocean carbon pumps: Analysis of relative strengths and efficiencies in ocean-driven atmospheric CO2 changes, in: Sundquist, E.T., Broecker, W.S. (Eds.), Geophysical Monograph Series. American Geophysical Union, Washington, D. C., pp. 99–110.

964 **Table 1:** Dynamics of carbon and nitrogen export fluxes at station A3 collected by the
965 sediment trap at 289 m.

			Fluxes (mmol m^{-2} d^{-1})			Contribution to annual export (%)	
Cup	**Start**	**Stop**	**POC**	**PON**	**POC:PON**	**POC**	**PON**
1	21/10/2011	04/11/2011	0.15±0.01	0.02±0.00	6.80±0.56	2.11±0.06	2.30±0.01
2	04/11/2011	18/11/2011	0.14 ±0.01	0.02±0.00	6.09±0.67	1.94±0.16	2.27±0.15
3	18/11/2011	02/12/2011	0.15±0.01	0.02±0.00	7.33±0.31	2.12±0.06	1.99±0.06
4	02/12/2011	12/12/2011	1.60±0.04	0.23±0.01	6.95±0.29	16.18±0.45	16.48±0.07
5	12/12/2011	22/12/2011	0.34±0.00	0.05±0.00	6.87±0.08	3.41±0.03	3.64±0.03
6	22/12/2011	01/01/2012	0.51±0.04	0.08±0.01	6.70±0.78	4.82±0.76	5.50±0.39
7	01/01/2012	11/01/2012	0.42±0.02	0.06±0.00	6.73±0.46	4.23±0.14	4.65±0.42
8	11/01/2012	25/01/2012	0.34±0.01	0.05±0.00	6.94±0.38	4.83±0.18	4.84±0.11
9	25/01/2012	08/02/2012	1.47±0.03	0.20±0.01	7.38±0.26	20.98±0.57	21.07±0.05
10	08/02/2012	22/02/2012	0.55±0.04	0.08±0.00	6.97±0.88	7.83±0.64	8.36±0.57
11	22/02/2012	31/05/2012	0.27±0.01	0.03±0.00	8.09±0.22	26.84±0.47	24.12±0.20
12	31/05/2012	07/09/2012	0.04±0.00	0.01±0.00	6.06±0.17	4.71±0.90	4.78±0.09
Annual export (mmol m^{-2} y^{-1})			98.24±4.35	13.59±0.30			

966

967

968 **Table 2:** Number of swimmer individuals found in each cup and swimmer intrusion rate
969 (number d^{-1}, *bold italic* numbers) for each taxa and for the total swimmers.

Cup	Copepod	Pteropod	Euphausiid	Ostracod	Amphipod	Cnidarian	Polychaete	Ctenophore	Siphonophore	Salp	Total
1	166	13	1	2	1	0	0	0	0	0	183
	12	***1***	***< 1***	***< 1***	***< 1***	***0***	***0***	***0***	***0***	***0***	***13***
2	55	0	0	0	0	0	0	0	0	0	55
	4	***0***	***0***	***0***	***0***	***0***	***0***	***0***	***0***	***0***	***4***
3	0	0	0	0	0	0	0	0	0	0	0
	0	***0***	***0***	***0***	***0***	***0***	***0***	***0***	***0***	***0***	***0***
4	113	0	0	0	0	0	0	0	0	0	113
	11	***0***	***0***	***0***	***0***	***0***	***0***	***0***	***0***	***0***	***11***
5	0	0	0	0	0	0	0	0	0	0	0
	0	***0***	***0***	***0***	***0***	***0***	***0***	***0***	***0***	***0***	***0***
6	540	0	1	0	2	5	1	4	1	0	554
	54	***0***	***< 1***	***0***	***< 1***	***< 1***	***0***	***0***	***0***	***0***	***55***
7	583	0	0	0	0	2	2	3	0	0	590
	58	***0***	***0***	***0***	***0***	***< 1***	***< 1***	***< 1***	***0***	***0***	***58***
8	686	33	2	2	8	5	1	4	0	0	741
	49	***2***	***< 1***	***< 1***	***1***	***< 1***	***< 1***	***< 1***	***0***	***0***	***52***
9	392	14	4	3	121	4	2	0	0	0	540
	28	***1***	***< 1***	***< 1***	***9***	***< 1***	***< 1***	***0***	***0***	***0***	***38***
10	264	69	1	2	18	11	0	2	0	0	367
	19	***5***	***< 1***	***< 1***	***1***	***1***	***0***	***< 1***	***0***	***0***	***26***
11	54	0	0	0	29	4	1	0	0	0	88
	1	***0***	***0***	***0***	***< 1***	***< 1***	***< 1***	***0***	***0***	***0***	***1***
12	1481	44	5	7	2	3	2	0	0	1	1544
	15	***< 1***	***< 1***	***< 1***	***< 1***	***< 1***	***< 1***	***0***	***0***	***< 1***	***15***

970

971

Table 3: Synthesis of estimates of POC fluxes at the base of, or under, the mixed layer at station A3 from the KEOPS 1 cruise.

Author	Method	Period	Depth (m)	POC flux (mmol m^{-2} d^{-1})
		KEOPS1		
Savoye et al., 2008	^{234}Th deficit	23 Jan – 12 Feb 2005	100	23 ± 3.6
			150	25.7 ± 3.6
			200	24.5 ± 6.8
Ebersbach and Trull, 2008	Drifting gel trap, optical measurements and constant C conversion factor	4 Feb 2005	200	23.9
		12 Feb 2005	100	5.3
			200	5.2
			330	0.7
			430	1
Jouandet et al., 2008	Annual DIC budget	Annual	MLD base	85
Trull et al., 2008b	Drifting sediment trap	4 Feb 2005	200	7.3-10
		12 Feb 2005		3-3.1
Jouandet et al., 2011	In situ optical measurement (UVP) and power function C conversion factor	22 Jan 2005	200	72.4
			330	27.2
			400	21.6
		23 Jan 2005	200	29.8
			330	26.8
			400	15.9
		12 Feb 2005	200	4.8
			330	5.6
			400	7.9
		KEOPS2		
Planchon et al., 2014	^{234}Th deficit, steady state model	20 Oct 2011	100	3.5 ± 0.9
			150	3.9 ± 0.9
			200	3.7 ± 0.9
		16 Nov 2011	100	4.6 ± 1.5
			150	7.1 ±1.5
			200	3.1 ± 0.6
	^{234}Th deficit, non steady state model	16 Nov 2011	100	7.3 ± 1.8
			150	8.4 ± 1.8
			200	3.8 ± 0.8
Laurenceau et al., 2014	Drifting gel trap, optical measurement of particles	16 Nov 2011	210	5.5
	Drifting sediment trap		210	2.2
Jouandet et al., 2014	In situ optical measurement (UVP) and power function C conversion factor	21 Oct 2011	200	0.2
			350	0.1
		16 Nov 2011	200	1.9
			350	0.3

974

975 **Figures captions**

976 **Figure 1.** Localization of the Kerguelen Plateau in the Indian sector of the Southern Ocean
977 and detailed map of the satellite-derived surface chlorophyll *a* concentration (MODIS level 3
978 product) averaged over the sediment trap deployment period. Sediment trap location at the A3
979 station is represented by a black dot, whereas the black circle represents the 100 km radius
980 area used to average the surface chlorophyll *a* time series. Arrows represent surface
981 geostrophic circulation derived from the absolute dynamic topography (AVISO product).
982 Positions of the Antarctic Circumpolar Current core (AAC core), the Polar Front (PF) and the
983 Fawn Through Current (FTC) are shown by thick black arrows. Grey lines are 500 m and
984 1000 m isobaths.

985 **Figure 2.** Schematic of the instrumented mooring line against vertical temperature profiles.
986 The sediment trap and the current meter/CTD sensor location on the mooring line are shown
987 by white circles. Temperature profiles performed during the sediment trap deployment (20
988 October 2011) are represented by grey lines. Black full line is the median temperature profile
989 from 12 casts realized on the 16 November 2011. Dashed black lines are the first and third
990 quartiles from these casts. The grey rectangle represents the Kerguelen Plateau seafloor. The
991 different water masses are Antarctic Surface Water (AASW), Winter Water (WW) and Upper
992 Circumpolar Deep Water (UCDW).

993 **Figure 3.** Hydrological properties recorded by the instrument mooring at station A3. a) depth
994 of the CTD sensor, b) salinity, c) potential temperature, d) line angle, e) current speed, grey
995 lines are raw data, black lines are low-pass filtered data with a Gaussian filter (40 hour
996 window as suggested by the spectral analysis), f) direction and speed of currents represented
997 by vectors (under sampled with a 5 hours interval) and g) wind rose plot of current direction

998 and intensities, dotted circles are directions relatives frequencies and colors refer to current
999 speed (m s^{-1}).

1000 **Figure 4.** Potential temperature/salinity diagram at station A3. Data are from the moored
1001 CTD (black dots), KEOPS1 (blue line) and KEOPS2 (red line). Grey lines are potential
1002 density anomaly. The different water masses are Antarctic Surface Water (AASW), Winter
1003 Water (WW) and Upper Circumpolar Deep Water (UCDW).
1004

1005 **Figure 5.** Power spectrum of the spectral analysis of a) depth time series and b) potential
1006 density anomaly time series. Pure red noise (null hypothesis) is represented by red dashed
1007 lines for each variable. The period corresponding to a significant power peak (power peak
1008 higher than the red noise) is written.

1009 **Figure 6.** Progressive vector diagram (integration of the current vectors all along the current
1010 meter record) calculated from current meter data at 319 m. The color scale refers to date.

1011 **Figure 7.** Seasonal variations of surface chlorophyll *a* and particulate organic carbon (POC)
1012 export. a) Seasonal surface chlorophyll concentration and 16 years climatology (Globcolour)
1013 averaged in a 100 km radius around the station A3 station The black line represents the
1014 climatology calculated for the period 1997/2013, whilst the green line corresponds to the
1015 sediment trap deployment period (2011/2012). b) POC flux (grey bars) and mass percentage
1016 of POC (red dotted line). Error bars are standard deviations from triplicates, bold italic
1017 numbers refer to cup number.

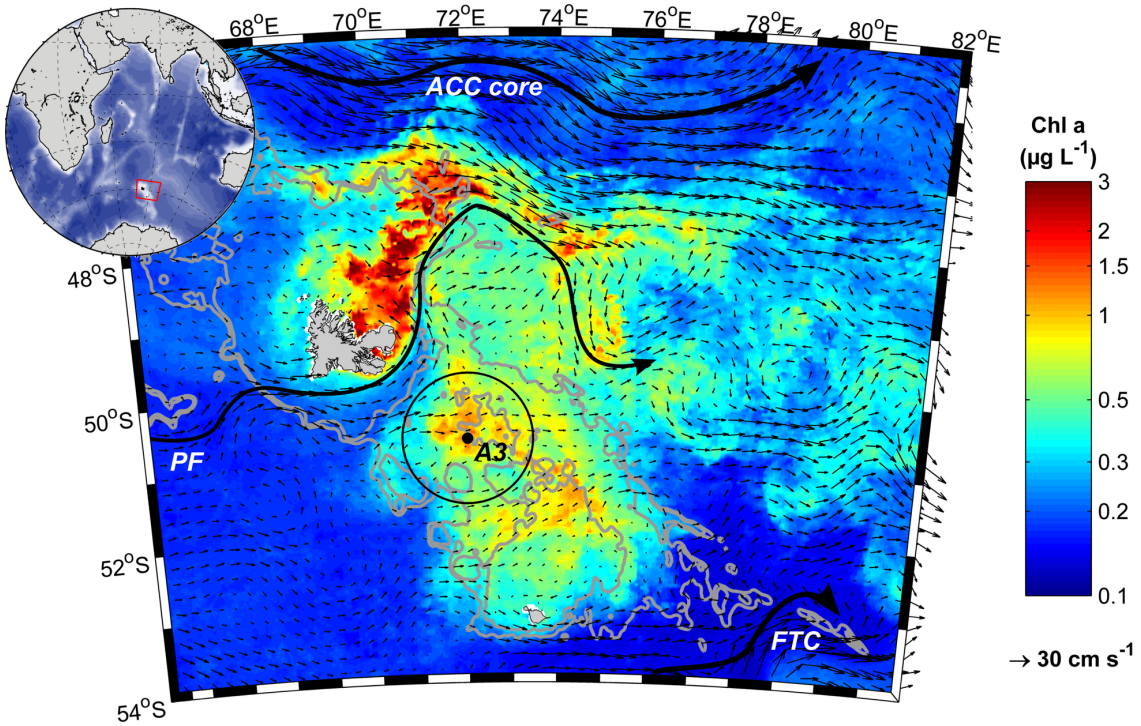

Figure 1.

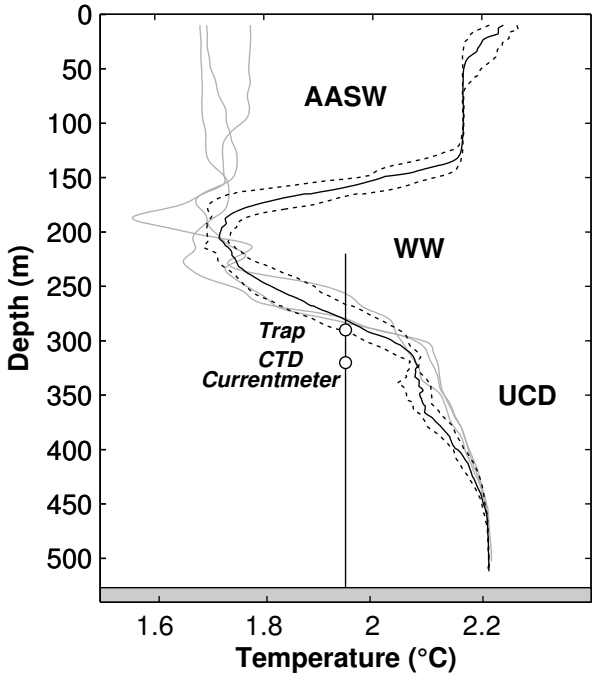

Figure 2.

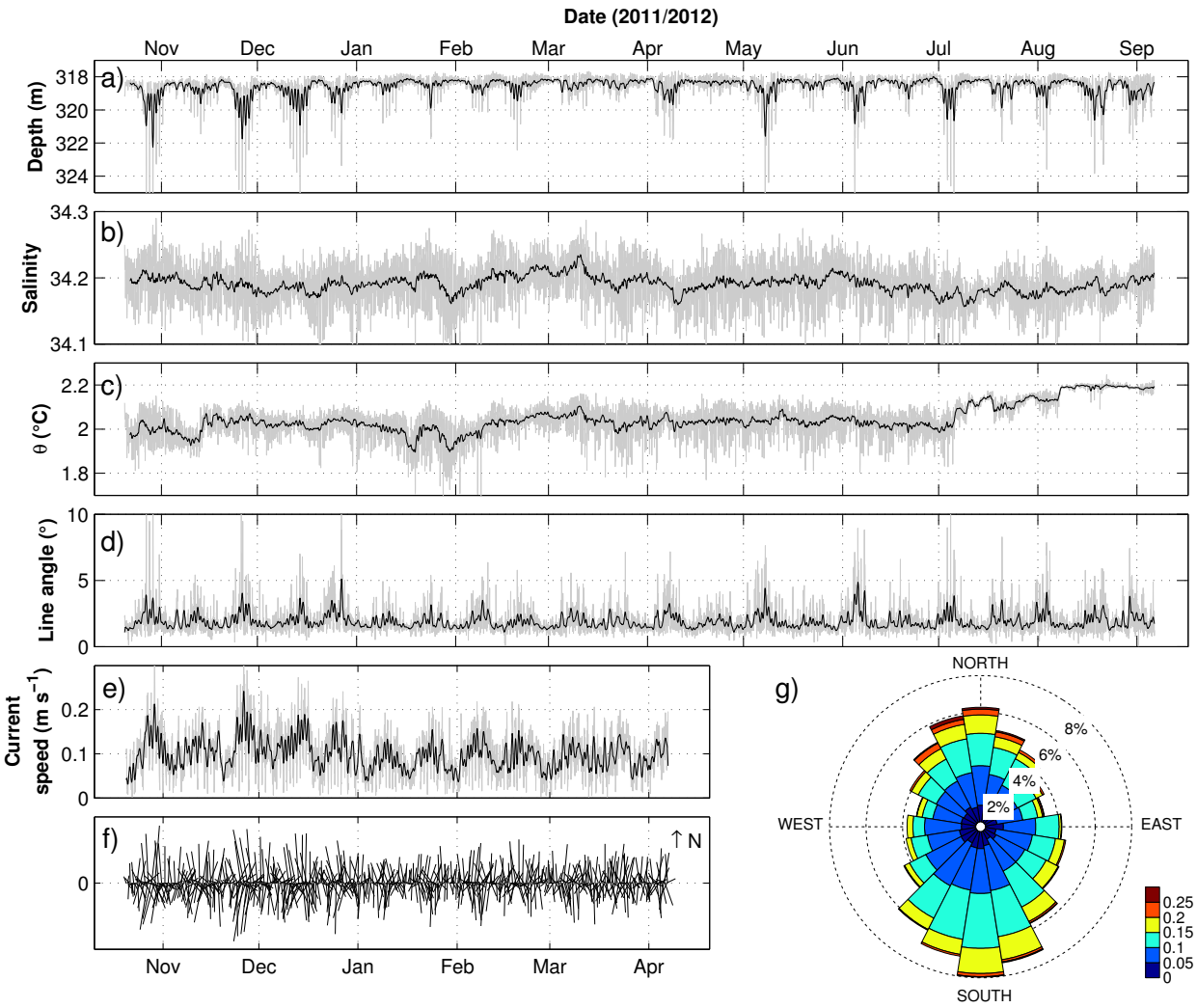
Date (2011/2012)
Nov
Dec
Jan
Feb
Mar
Apr
May
Jun
Jul
Aug
Sep
a)
Depth (m)
318
320
322
324
b)
Salinity
34.3
34.2
34.1
c)
θ (°C)
2.2
2
1.8
d)
Line angle (°)
10
5
0
e)
Current speed (m s^{-1})
0.2
0.1
0
f)
0
↑ N
Nov
Dec
Jan
Feb
Mar
Apr
g)
NORTH
8%
6%
4%
2%
WEST
EAST
SOUTH
0.25
0.2
0.15
0.1
0.05
0

Figure 3.

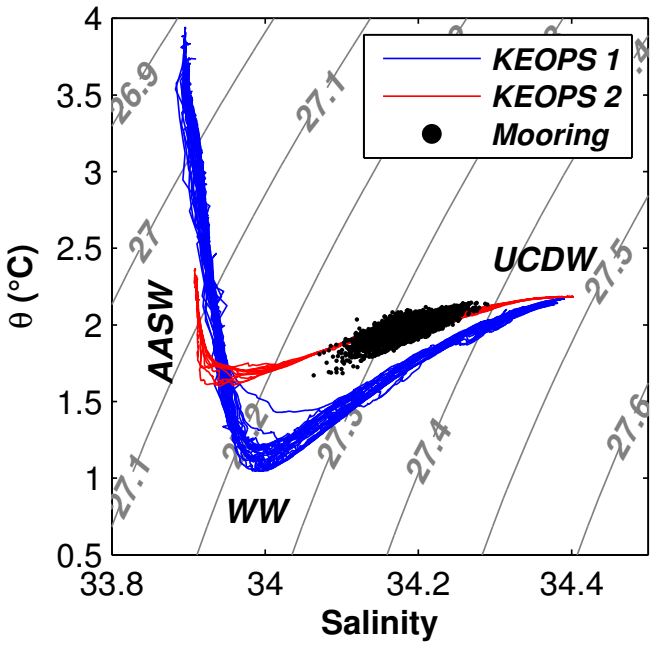

Figure 4.

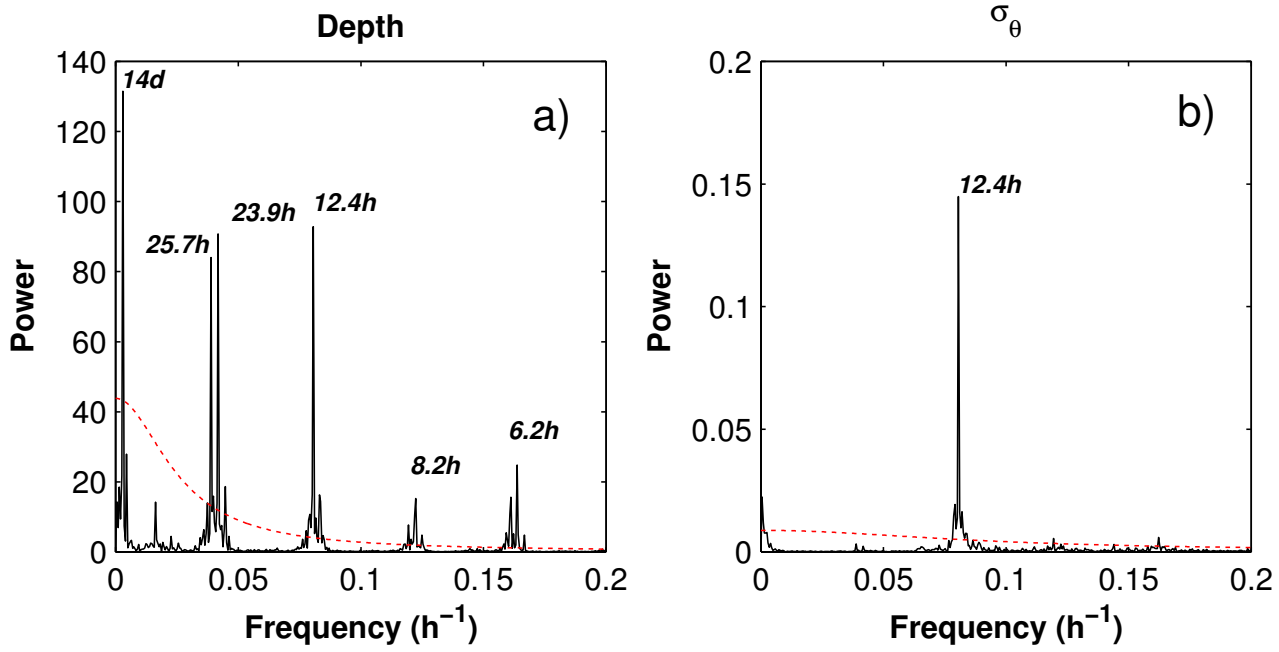

Figure 5.

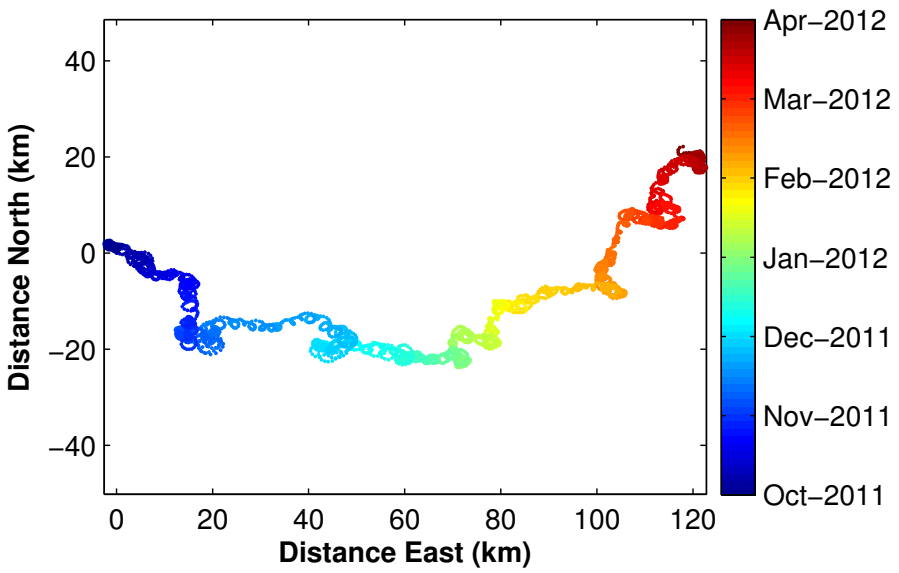

Figure 6.

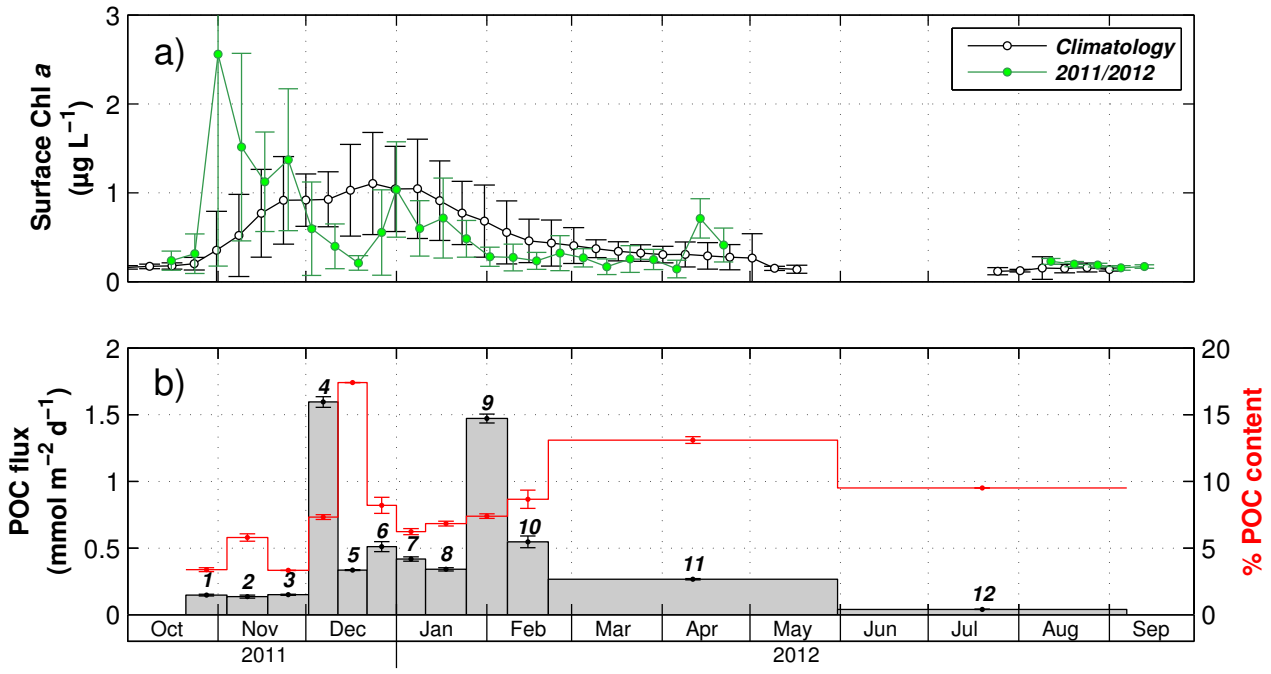

Figure 7.